

δ -Aminolevulinic acid and its methyl ester induce the formation of Protoporphyrin IX in cultured sensory neurones

B. Novak · R. Schulten · H. Lübbert

Received: 20 July 2011 / Accepted: 14 August 2011 / Published online: 25 September 2011
© Springer-Verlag 2011

Abstract Application of δ -aminolevulinic acid (ALA) or its methyl ester (MAL) onto cutaneous tumours increases intracellular Protoporphyrin IX (PpIX), serving as photosensitizer in photodynamic therapy (PDT). While PDT is highly effective as treatment of neoplastic skin lesions, it may induce severe pain in some patients. Here, we investigated ALA and MAL uptake and PpIX formation in sensory neurones as potential contributor to the pain. PpIX formation was induced in cultured sensory neurones from rat dorsal root ganglion by incubation with ALA or MAL. Using inhibitors of GABA transporters (GAT), a pharmacological profile of ALA and MAL uptake was assessed. GAT mRNA expression in the cultures was determined by RT-PCR. Cultured sensory neurones synthesised Protoporphyrin IX (PpIX) from extracellularly administered ALA and MAL. PpIX formation was dose- and time-dependent with considerably different kinetics for both compounds. While partial inhibition occurred using L-arginine, PpIX formation from both ALA and MAL could be fully blocked by the GABA-Transporter (GAT)-2/3 inhibitor (S)-SNAP 5114 with similar K_i (ALA: $195 \pm 6 \mu\text{M}$; MAL: $129 \pm 13 \mu\text{M}$). GAT-1 and GAT-3 could be detected in sensory neurons using RT-PCR on mRNA level and using [^3H]-GABA uptake on protein level. Cultured sensory neurones take up ALA and MAL and synthesize PpIX from both, enabling a direct impact of photodynamic therapy on

cutaneous free nerve endings. The pharmacological profile of ALA and MAL uptake in our test system was very similar and suggests uptake via GABA and amino acid transporters.

Keywords Delta-aminolevulinic acid · Methyl-aminolevulinic acid · Photodynamic therapy · Cellular uptake · Protoporphyrin IX · GABA transporters (GAT) · Amino acid transporters

Abbreviations

ALA	δ -Aminolevulinic acid
BGT-1	Betaine-GABA transporter 1
BNPP	Bis(<i>p</i> -nitrophenyl) phosphate sodium salt
DMEM	Dulbecco's modified Eagle's medium
DRG	Dorsal root ganglion
F12	Nutrient mixture F12
GABA	γ -Aminobutyric acid
GAT	GABA transporter
L-Arg	L-Arginine
MAL	ALA-methyl ester
PpIX	Protoporphyrin IX
RFU	Relative fluorescence units
(S)-SNAP 5114	1-[2-[Tris(4-methoxyphenyl)methoxy]ethyl]-(S)-3-piperidinecarboxylic acid

B. Novak · R. Schulten · H. Lübbert (✉)
Department of Animal Physiology,
Faculty of Biology and Biotechnology, Ruhr-University Bochum,
Building ND 5/122, Universitätsstr. 150,
44780 Bochum, Germany
e-mail: h.luebbert@biofrontera.com

B. Novak
e-mail: Ben.Novak@rub.de

R. Schulten
e-mail: Roxane.Schulten@rub.de

Introduction

In photodynamic therapy (PDT), the heme precursor Protoporphyrin IX (PpIX) serves as a photosensitizing agent for the therapy of skin tumours, psoriasis and related conditions (MacCormack 2008). PpIX can be generated inside target cells by application of its precursor δ -aminolevulinic acid (ALA) or an ALA ester (e.g. methyl

aminolevulinic acid, MAL). Interestingly, PpIX accumulation in diseased cells is stronger than in healthy ones (Collaud et al. 2004). This has been attributed to an enzymatic imbalance between PpIX generating and catabolising enzymes (Van Hillegersberg et al. 1992) on the one hand or to an altered tissue penetration and plasma membrane uptake on the other (e.g. Rud et al. 2000; Wennberg et al. 2000; Collaud et al. 2004). ALA-derived PpIX accumulates inside mitochondria, where, upon illumination, a type II photochemical reaction provides highly reactive singlet oxygen, which will eventually destroy the cell (Almeida et al. 2004).

One drawback of this otherwise very effective therapeutic approach is pain experienced by many patients during the illumination phase (Grapengiesser et al. 2002; Ericson et al. 2004; Kasche et al. 2006; Lindeburg et al. 2007). It has been speculated that the origin of this pain is a direct photodynamic influence on epidermal C fibres, although there is no direct evidence so far. An indispensable prerequisite for a direct impact would be an uptake of ALA or its esters and subsequent PpIX formation in neuronal cells. In this study, we have chosen cultured sensory neurones from rat dorsal root ganglia (DRG) as a test system to analyse ALA and MAL uptake into said structures.

Various pathways have been described for ALA and MAL membrane transition. Several studies were able to attribute it to GABA transporters in various tumour cell lines (Rud et al. 2000; Bermudez et al. 2002; Rodriguez et al. 2006). Emphasis has been on the observation that uptake rates for ALA and its esters are markedly different for these transporters (Rud et al. 2000; Rodriguez et al. 2006). Furthermore, peptide and amino acid transporters have been shown to be capable of ALA transport (Doring et al. 1998; Novotny et al. 2000; Whitaker et al. 2000; Frolund et al. 2010) and some authors discuss passive diffusion through membranes even for the very hydrophilic ALA (Bermudez et al. 2002).

With the plethora of possible uptake pathways in different test systems and cell lines, it seems likely that there is no unique mode of uptake. It may rather be dependent on the specific composition of transport systems in a given cell type (Casas et al. 2002). Therefore, only a study in primary sensory neurones can clarify whether ALA and MAL uptake into sensory neurones exists and whether different or the same transporter proteins account for it.

GABA transporters located in the plasma membrane belong to the solute carrier family 6 (SLC6) and provide sodium and chloride dependent transport of GABA across cell membranes (Alexander et al. 2009). Four different transporter subtypes could be cloned in human and rat (GAT-1 to GAT-3 and BGT-1; Sarup et al. 2003; also often referred to as BETA transporters). While their expression profile for the brain and several other organs was thoroughly investigated (e.g. Borden

1996; Conti et al. 1999; Liu et al. 1999; Minelli et al. 2003), information on their expression in the DRG is rather sparse. Only one report (Shoji et al. 2010) showed GAT-3 expression in the rat nodose ganglion by immunohistochemistry.

We have used a fluorescence-based non-radioactive multiplate assay to analyse PpIX formation in DRG sensory neurone cultures after incubation with PpIX precursors (ALA and MAL). Both compounds induced an increase in PpIX-like fluorescence in DRG cultures, which is dependent on synthesis time and precursor concentration. Co-incubation with substrates of GABA transporters led to a decrease in PpIX formation from both ALA and MAL. The GAT-2/3 inhibitor (*S*)-SNAP 5114 (~80-fold over GAT-1; Borden 1996) at high concentrations provided an almost complete block of PpIX formation from ALA as well as MAL. Further investigations by RT-PCR revealed the expression of GAT-1 and GAT-3, but not GAT-2, in our cultures. Investigations using [³H]-labelled GABA further validated a GAT-3 activity in sensory neurons and its predominant role in GABA uptake. In addition, a competitive inhibition by L-arginine could be reported. Application of an inhibitor of extracellular carboxyesterases revealed that MAL is partly converted to ALA before neuronal uptake in our test system. Our results clearly indicate that a direct photodynamic action of PpIX in epidermal sensory nerve endings must be envisaged. Both ALA and its methyl ester MAL give rise to PpIX generation in sensory neurones, while they could be clearly shown as non-neurotoxic in a neurite outgrowth assay.

Methods

In this paper, drug and molecular target nomenclature follows Alexander et al. (2009).

Chemicals

ALA hydrochloride was obtained from Biofrontera Pharma GmbH (Leverkusen, Germany), MAL hydrochloride, guvacine hydrochloride, γ -aminobutyric acid (GABA), β -alanine, (*S*)-SNAP 5114 and all amino acids applied in this study were obtained from Sigma Chemical Co. (St. Louis, MO). All chemicals were obtained in the purest available grade (not below $\geq 98\%$).

The primary antibody against β III-tubulin was obtained from Sigma Chemical Co. (Clone 2G10; mouse monoclonal), sheep- α -CGRP (Calcitonin gene-related peptide) polyclonal antibody was obtained from Biomol GmbH (Hamburg, Germany) and isolectin B4 from Gryffonia simplicifolia was obtained from Invitrogen (Carlsbad, CA). Corresponding secondary antibodies and Avidin-Fluorescein D conjugate were purchased from Vector Labs (Burlingame, CA).

All other chemicals for buffer preparation and cell culture were of analytical grade and obtained from Sigma Chemicals Co..

Preparation of dorsal root ganglia and DRG cell culture

Dorsal root ganglia were prepared from 3- to 7-day-old Wistar rat pups based on the method described for mice by Malin et al. 2007 with minor variations. In short, rats were decapitated and the roof (dorsal portion) of the vertebral column was removed. Ganglia were then dissected out individually starting at the most cervical ganglion and proceeding towards the sacral end. Around 40 cervical to lumbal ganglia could be obtained per animal and were collected in ice-cold Leibovitz L-15 medium (Sigma). For enzymatic digestion, the tissue was then transferred to prewarmed L-15 medium containing 0.1% (w/v) collagenase type I (Worthington) and 0.25% (w/v) trypsin (Invitrogen) and incubated for 45 min at 37°C. Afterwards, the digested ganglia were centrifuged for 3 min at 163×g. The pellet was resuspended in prewarmed culture medium (DMEM/F12 1:1, Invitrogen) supplemented with 10% (v/v) Normal Horse Serum (Gibco by Invitrogen), 100 U/ml penicillin and 100 µg/ml streptomycin (Gibco) and triturated several times through the tip of a fire polished glass pipette. Cell suspension was then filtered through a 100-µm cell strainer (BD Biosciences, Franklin Lakes, NJ), and the strainer was rinsed with additional 10 ml of culture medium. The resulting suspension, cleared of tissue chunks and undigested fibres, was now centrifuged for 12 min at 17×g. After removal of the supernatant, the resulting pellet was carefully resuspended in 1 ml culture medium, containing 50 ng/ml Nerve Growth Factor (NGF, 2.5S from purified from mouse, Promega, Madison, WI). The cell yield was quantified using a Neubauer chamber, and cells at desired densities were plated on poly-D-lysine (100 µg/ml in phosphate buffered saline (PBS)) and Laminin (2.6 mg/ml in PBS)-coated dishes. Cells were maintained in culture for 48 h in the incubator in a humidified atmosphere at 37°C, 5% CO₂. A 50% medium exchange was performed 24 h after plating.

Immunocytochemistry and isolectin staining

For immunocytochemistry cells grown on 10-mm diameter glass coverslips for 48 h were fixed using 4% paraformaldehyde (PFA) for 20 min at 4°C. Cells were then washed three times using 0.01 M PBS (Gibco), and unspecific binding was blocked using a 5% solution of serum from the species in which the secondary antibody was raised (in the double-labelling situation, 5% foetal calf serum was used) diluted in 0.01 M PBS. This solution also contained 0.1% Triton X-100 (Sigma). Blocking solution was left on the cells for 45 min at room temperature. Subsequently, one of the following antibodies/labelling compounds was used in the given dilution: mouse monoclonal α - β III-tubulin (1:1000), sheep polyclonal α -CGRP (1:2000) or isolectin B4 (IB4) from *Griffonia simplicifolia* (1:250). All antibodies were diluted in 0.01 M PBS. Whenever IB4 was used alone or in combination, 1 µM CaCl₂ was added to the PBS. Cells were incubated together with the primary antibody/labelling compound at 4°C overnight. On the following day, cultures were washed three times with 0.01 M PBS and incubated with the secondary antibody (alone or in combination) for 1 h at RT. In case a biotinylated secondary antibody was used, cells were incubated in avidin-Fluorescein D (AviFiTC; Vector Labs) for another 45 min at RT. A nuclear stain was performed using 10 µg/ml Hoechst 33342 (Sigma) in 0.01 M PBS for 20 min at RT and coverslips were mounted on Superfrost® slides (Thermo Fisher Scientific, Waltham, MA) using VectaShield mounting medium (Vector Labs). Table 1 gives an overview of the antibodies used.

Uptake of ALA and MAL and PpIX measurement

For the measurement of either ALA or MAL derived PpIX, cell cultures were incubated with ALA/MAL either in DMEM/F12 without serum and Phenol Red containing 50 ng/ml NGF or the uptake buffer according to Gederaas et al. 2001 (10 mM HEPES; 150 mM NaCl; 1.2 mM CaCl₂; 0.64 mM MgCl₂; 6 mM KOH; 5 mM Glucose, pH adjusted to 7.4 with 5 M NaOH) at 37°C for 30 min in the incubator. The pH of all ALA/MAL solutions was adjusted to 7.4

Table 1 Antibodies and dilutions used for immunocytochemistry

	Antigen	Antibody/detection reagent	Source	Dilution
Primary	β tubulin isotype III	Mouse-anti- β III-tubulin monoclonal (clone SDL.3d10)	Sigma	1:1000
	Calcitonin gene-related peptide	Sheep-anti-CGRP polyclonal	Biomol	1:2000
	N-acetyl-D-galactosamine	Isolectin B4	Invitrogen	1:250
Secondary	Mouse IgG (Fc)	CY3-conjugated-horse-anti-mouse polyclonal	Jackson ImmunoResearch	1:400
	Sheep IgG (Fc)	Biotinylated-rabbit-anti-mouse polyclonal	Jackson ImmunoResearch	1:300

using 5 M NaOH. After the uptake step, the ALA/MAL containing medium was omitted and the cells were washed once with DMEM/F12 without serum, Phenol Red and growth factor. Then, pre-warmed DMEM/F12 without serum and indicator but containing 50 ng/ml NGF was added. DMEM/F12 without serum and indicator, but with NGF, served as a control for non-loaded cells, representing the *vehicle-control* condition. Synthesis durations of 0 h (measurement directly after the 30 min uptake period), 1, 2 and 4 h were performed. When microscopic studies of PpIX synthesis were carried out, cells (cultures grown for 48 h on 30-mm glass coverslips at a density of 30,000 cells per glass) were transferred to an inverted microscope (Leica DMI 4000B; Leica, Wetzlar, Germany) and PpIX fluorescence was assessed employing a custom built filter cube containing a 420-nm excitation and a 620-nm emission band-pass filter set as well as a 470-nm beam splitter. A Leica EL6000 containing a 120-W mercury short arc lamp served as light source. Cells of clear neuronal morphology were identified in phase contrast optics and immediately examined for PpIX fluorescence. Vehicle-treated cultures served as a control for endogenous fluorescence at the given parameters.

For validation of PpIX fluorescence in nociceptor subtypes, neurones were seeded on dishes provided with a custom made 500 μm grid in order to localize and identify individual cells. Cultures were then subjected to the abovementioned uptake procedure and subsequently analysed microscopically. Cultures were then fixed and stained for β III-tubulin and CGRP or IB4 respectively as specified above.

When PpIX synthesis was measured in 96-well plates, 5,000 neurones were plated per well in 100 μl culture medium, grown for 48 h and incubated with ALA as described above. In these assays, all conditions were analysed in triplicates. At the end of the given synthesis durations, medium was removed from the cells, and 20 μl of a lysis buffer (125 mM Tris/HCl, pH 7.8; 2 mM DTT; 2 mM CDTA; 10% (v/v) Glycerol; 1% (v/v) Triton X-100; all Sigma) were added for 5 min. The buffer had beforehand been checked not to interfere with PpIX fluorescence measurements. Cultures were exposed to gentle planorbital shaking during lysis. Cell lysis was controlled under the microscope. When cultures were lysed completely, 80 μl of PpIX extraction solution (50% methanol; 35.7% distilled water; 14.3% perchloric acid (presolved to 70% in water) all v/v) were added and cells were again placed on a planorbital shaker for 10 min. Cell extracts were then transferred into a black-walled 96-well plate (Greiner, Bio-one) in order to assess PpIX fluorescence. These measurements were performed in a Mithras LB 940 multi-plate reader (Berthold Technologies GmbH & Co. KG, Bad Wildbad, Germany), employing a 390-nm excitation—620-nm emission filter set taking an integrated

read-out period of 10 s per well. A mixture of 20 μl lysis buffer and 80 μl extraction buffer served as background to be subtracted from all measurements. Data are depicted as relative fluorescence units (RFU).

ALA and MAL uptake in the presence of potential competitors

In order to screen for uptake pathways, DRG cultures were co-incubated with ALA or MAL and potential candidates for competitive inhibition of uptake routes. The experiments were performed in 96-well plates. Uptake measurements were carried out using ALA at a concentration of 0.6 mM and MAL at a concentration of 1.8 mM. ALA or MAL were added to the cells in the presence of the inhibitory drug at four test concentrations. The uptake duration was always 30 min. Subsequently, cultures were processed as described above, with the PpIX synthesis phase kept constant at 2 h. Read-out parameters and control conditions were identical to standard uptake experiments without inhibitors. All measurements were performed as triplicates and background values of lysis and extraction buffer were subtracted from all obtained values. When bis(*p*-nitrophenyl) phosphate sodium salt (BNPP) was used to inhibit carboxyesterases, DRG neurone cultures were either pre-incubated with 200 μM BNPP for 15 min in uptake buffer and MAL or ALA were added with BNPP still present for the standard 30 min uptake interval, or BNPP was added together with MAL and was present during the uptake interval. Synthesis time in these experiments was also 2 h, and samples were processed further as described above.

Gene expression analysis

For gene expression analysis, total RNA was extracted from 5×10^5 DRG neurones cultured as described above as well as neocortical or liver tissue from Wistar rat pups at postnatal day 5. RNA extraction was performed using the Trizol[®] method as described previously (Wendt et al. 2007). Fifteen milligrams of total RNA were subjected to cDNA synthesis employing random hexamer primers and M-MLV reverse transcriptase and using the Fermentas RevertAid[®] cDNA synthesis kit (Fermentas, St. Leon-Rot, Germany) according to the manufacturers' instructions (+RT). As negative controls, samples of RNA were subjected to this reaction with the reverse transcriptase being omitted (−RT).

Polymerase chain reactions for expression analysis were carried out using oligonucleotide primers that were designed to span introns in order to exclude genomic DNA contaminations. Primer sequences are displayed in Table 2.

PCR amplifications were performed in an automated thermal cycler (RoboCycler Gradient 96; Stratagene Europe,

Table 2 Oligonucleotide primers used for RT-PCR

Gene	Bases	Oligonucleotide sequences (5'→3')	Product size (bp)
GAT-1	757–776 903–922	GGCTAGACAAGCCAGGACAG CCACGGAAGAACAGGATGAT	166
GAT-2	18–37 183–202	CATCCGGTAGAACGGAAAGA TCCTCCACCTTCTCCATGAC	185
GAT-3	398–417 569–588	ATGCAACACAGGTGATCGAG CTGCAGGGACACATGACTGT	191

Primers were designed using Genebank sequences and Primer3 Software. Optimal primer pairs were chosen and compared to other cloned sequences via a BLAST search

Amsterdam, The Netherlands) with an initial 5 min denaturation step at 95°C, followed by 35 cycles comprising a 45-s denaturation step at 95°C, a 45-s annealing step at 58°C (for GAT-3) or 60°C (for GAT-1 and 2) and a 30-s elongation step at 72°C and a final elongation at 72°C for 3 min. All control samples (–RT) were processed in the same way in parallel to the cDNA samples (+RT). PCR products were separated by electrophoresis in a 2% agarose gel stained with 0.1 mg/ml ethidium bromide. A 100-bp DNA ladder (BioRad Laboratories GmbH, Munich, Germany) was used as a size standard. Gels were documented using a GelDoc system (BioRad) and corresponding software.

Uptake of radioactively labelled GABA

For uptake experiments using [³H]-labelled GABA, the method described for [¹⁴C]-GABA in Rodriguez et al. 2006 was used with minor variations. In short, solutions of unlabelled GABA were made using the uptake buffer described by Gederaas et al. 2001. γ -[2,3-³H(N)]-aminobutyric acid (Perkin Elmer, Waltham, MA) was added to achieve a radioactive concentration of 0,064 MBq ml⁻¹ and a total GABA concentration of 0.2 mM. Measurements were performed in 96-well plates. Cells were preincubated with potential inhibitors in the abovementioned buffer for 15 min at 37°C to assure previous binding to their targets. Afterwards, radiolabelled GABA was added so that the final concentration was 0.1 mM. Uptake was carried out for 30 min at 37°C. Afterwards, the cells were washed four times using ice-cold buffer containing 1 mM GABA to stop the uptake and to displace unspecifically bound [³H]-GABA. Afterwards, cells were lysed using 30 μ l 0.1 M NaOH and lysates were transferred to 96-well filterplates (Perkin Elmer), dried, provided with 30 μ l scintillation fluid (Microscint 0; Perkin Elmer) and measured in an appropriate scintillation counter (TopCount NXT; Packard). All measurements were performed as triplicates.

Neurotoxicity assay—morphometric analysis

For analysis of neurotoxicity, an assay investigating neurite length was used. Neurons cultured in 24-well plates on 10-mm diameter glass coverslips were treated with either 6 mM ALA

or MAL for 30 min and then were allowed to synthesize PpIX for either 2 or 4 h. Cells were then PFA-fixed and processed using a mouse monoclonal anti- β III-tubulin antibody as described above, while the staining was revealed by 3,3'-diaminobenzidine (Sigma). All experiments were repeated independently three times, and in each single experiment, three microscopic view fields were chosen per coverslip at random and the length of the longest neurites of all sampled neurons was measured using ImageJ software (NIH, Bethesda, MD; v. 1.41o).

Data analysis

Immunocytochemical stainings were visualized under an inverted microscope (Leica DMI 4000B), with fluorescence illumination being provided by the EL6000 light source, using FiTC, TriTC and Hoechst optimized filter sets. Images were captured by a camera system (DFC 350 FX, Leica, Wetzlar, Germany) and a computer equipped with the Leica Application Suite v. 2.8.4 software (Leica, Wetzlar, Germany). For final output, images were processed using Adobe® PhotoShop®CS v. 8.0.1.

Raw datasets from all experiments were imported to Microsoft Excel 2007 for calculation, further processing and illustration. For non-linear curve fits Origin® 8.1G software was used. The applied fitting functions were employed as suggested by the fitting wizard for non-linear curve fits. Functions were: *Hyperbolic* and *Dose-response* for finding EC₅₀ and *Hill1 equation* for finding IC₅₀. Cheng-Prusoff correction was carried out using the following equation (Cheng and Prusoff 1973):

$$pK_i = -\log ([IC_{50}] / (1 + ([Agonist] / [EC_{50}])))$$

Statistical analysis

For statistical testing of significant differences between datasets, WinSTAT for Microsoft Excel (v. 2007.1) and Sigma Stat (v. 3.5) software were used. For comparison of two groups, Student's *t* test was applied whenever the criteria for normality and equality of variance were met. In all other cases, Mann-Whitney *U* test for comparison of

two groups and Kruskal–Wallis ANOVA on ranks with subsequent Dunn's post-test for multiple comparisons were exerted. Significance criteria for rejection of the null hypothesis were reached at $p \leq 0.05$.

Results

Test system characterisation

Preparation of cell cultures from postnatal rodent dorsal root ganglia will yield a heterogeneous *in vitro* system comprising different types of sensory neurones (mechano-, proprio- and nociceptors) and non-neuronal cells such as Schwann cells and fibroblasts (Gilbert and McNaughton 1997; Andersen et al. 2003; Malin et al. 2007). C-type neurones extending processes into the epidermal layer are of special interest in this study's context. One can differentiate neuropeptide positive and negative C-type sensory neurones (Lawson 2002), both of which have been reported to innervate epidermal layers (Priestley et al. 2002; Lumpkin and Caterina 2007). We have aimed at estimating the neuronal content of our mixed cultures and at ascertaining the presence of neuropeptide positive (in this case, calcitonin gene-related peptide positive, CGRP+) and negative (but isolectin B4 positive, IB4+) neurones by means of immunocytochemistry. By staining neuronal cells with a monoclonal antibody against β III-tubulin and a Hoechst counter stain, the neuronal content in the culture system could be estimated as 9% (Fig. 1, A; graph in Fig. 1, D). Both types of nociceptive C-type sensory neurones could be detected in the cultures (Fig. 1, B, C). A quantification of the proportion of potentially nociceptive neurones (CGRP or IB4+) revealed that 12% of all neurones were IB4+ and 32% were CGRP+. Additionally we saw that reactivity towards IB4 and immunoreactivity towards CGRP antibodies are mutually exclusive characteristics here. In total, almost half of the neurones in our culture system can be regarded as potential nociceptors.

Microscopic evidence for ALA- and MAL-induced PpIX-like fluorescence in DRG cultures

As we deal with a heterogeneous culture system, we had to characterize the cell types displaying increased PpIX-like fluorescence on a microscopic single cell level following ALA/MAL incubation. Cell cultures were first loaded with ALA or MAL for 30 min, then washed and subsequently allowed to synthesize PpIX for 4 h. PpIX-like fluorescence was then visualized as described under [Methods](#). Greyscale photomicrographs are depicted in Fig. 2. Figure 2b shows the autofluorescence of cells that were not incubated with any compound. Only a weak fluorescence is visible. When

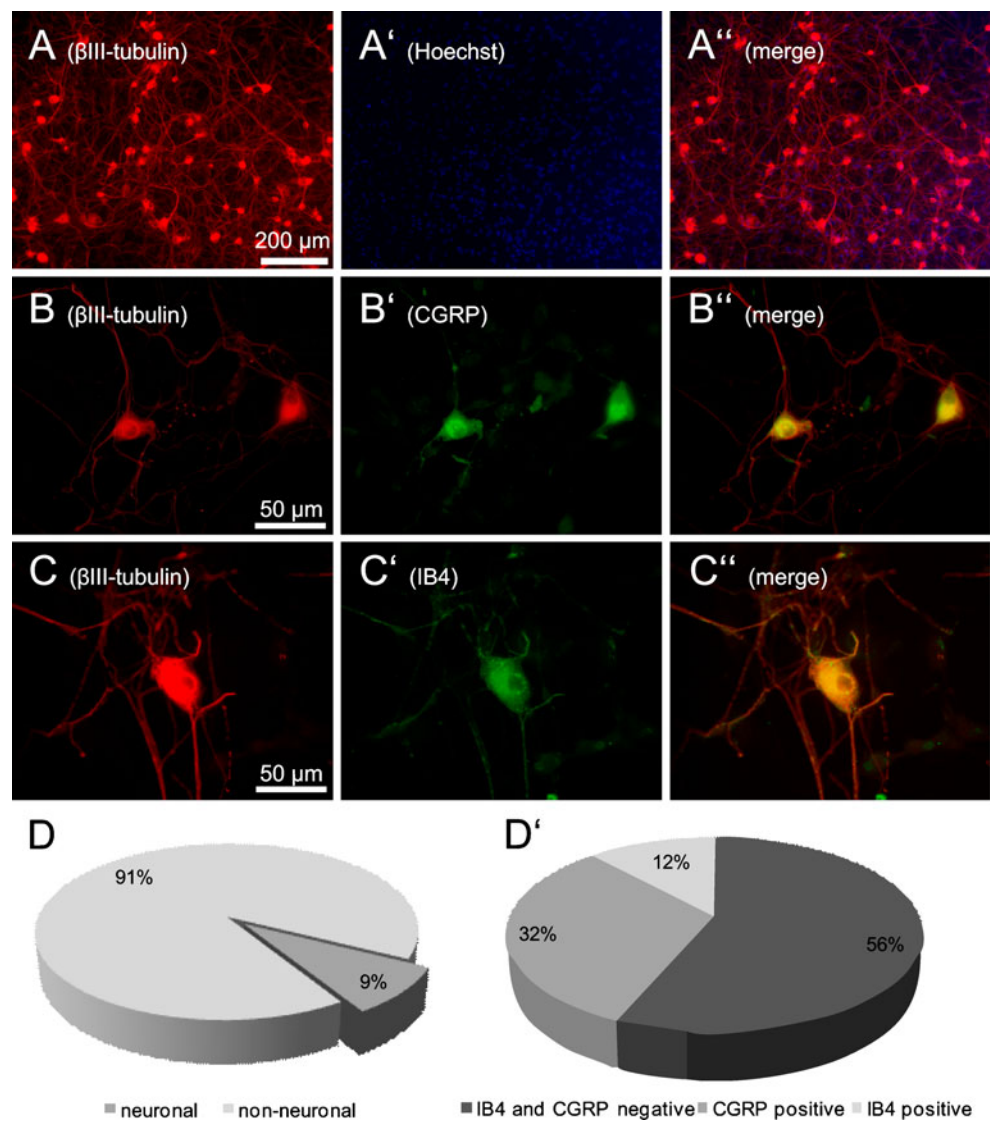
incubating neurone cultures with either 6 mM ALA or 6 mM MAL for 30 min and allowing a synthesis interval of 4 h, cells with clear neuronal morphology revealed much stronger PpIX-like fluorescence than under control conditions (Fig. 2a, c). Neuronal morphology was assessed under phase contrast microscopy, where PNS neurones exhibit rounded to oval-shaped cell bodies with a phase-bright rim and bear fine processes. These features match the cells highlighted in Fig. 2a, c. For the ALA-loaded cultures, fluorescence was also analysed for the remaining cell types in more detail. Flat, anamorphous and phase dark cells were likely to be fibroblasts. These cells exhibited only weak PpIX-like fluorescence (Fig. 2a; middle panel) compared to neighbouring neurones. Cultured Schwann cells can be recognized by a needle-like appearance with a slim or triangular soma and few processes. When evaluating PpIX-like fluorescence in these cells, no evidence for increased PpIX-levels could be detected (Fig. 2a; lowest panel). For MAL, an equal cellular distribution pattern could be described (compare Fig. 2c). Summing up, neurones appear to be the main contributors to PpIX-like fluorescence in mixed cultures incubated with ALA or MAL.

For an additional validation of PpIX synthesis in nociceptive neurones, we fixed neurone cultures after the microscopic assessment of PpIX production and conducted the staining for CGRP or IB4 as reported above. Furthermore, the neuronal identity of the PpIX producing cells was clarified using the β III-tubulin antibody at the same time. The results are presented in Fig. 3. It can be confirmed that on the one hand, β III-tubulin positive cells (i.e. neurones) synthesize PpIX from ALA and MAL and that PpIX synthesis from both pro-drugs also occurs in cells bearing nociceptor characteristics. PpIX production is not restricted to nociceptive C-fibre neurones but seems to take place in other neurone types as well.

Analysis of dose and time dependence of ALA/MAL-induced PpIX

To elucidate the dose and time dependence of PpIX formation after loading the cells with either ALA or MAL, cell cultures were incubated for 30 min with different ALA or MAL concentrations (0, 0.6, 1.8 or 6 mM). Cultures were then either washed and incubated further for 1, 2, 4 and 24 h, after which PpIX was determined (Fig. 4) or PpIX was determined immediately after uptake. The incubation of DRG neurone cultures with ALA or MAL resulted in an increased PpIX fluorescence in almost every condition. Directly after the uptake, fluorescence values were similar for all applied ALA or MAL concentrations and reached a maximum of around 200 RFU above background (Fig. 4a). When allowing the cultures to synthesize PpIX for one additional hour after the 30 min

Fig. 1 Immunocytochemical characterization of the cell cultures. Dissociated cells from the rat dorsal root ganglion were grown for 48 h and stained for a general neuronal and subtype markers. *A* Immunocytochemical staining of DRG cells with the neurone-specific antibody against β III-tubulin reveals a neuronal population while (*A'*) additional Hoechst staining clearly proves the existence of non-neuronal cells. The merge picture (*A''*) gives an estimate of the neuronal proportion of the total culture. In order to identify peptidergic nociceptors, co-expression of β III-tubulin (*red*) and CGRP (*green*) was analysed. Cells expressing both antigens are documented in (*B–B''*). Non-peptidergic nociceptive neurones were co-stained with β III-tubulin (*red*) and isolectin B4 (*green*) from *G. simplicifolia*. *C–C''* prove the existence of cells of this nociceptor subtype in the cultures. The pie charts in *D* and *D'* represent the quantification of neuronal cells and of nociceptor subtypes, respectively (from $n=3$ independent cultures)



uptake (Fig. 4b), clear saturation curves could be plotted. With only minor differences between ALA and MAL, saturation of PpIX formation was reached at ALA or MAL concentrations of 1.8 mM. With ALA, the maximum fluorescence level was 1,155 RFU, with MAL it was 1,010 RFU.

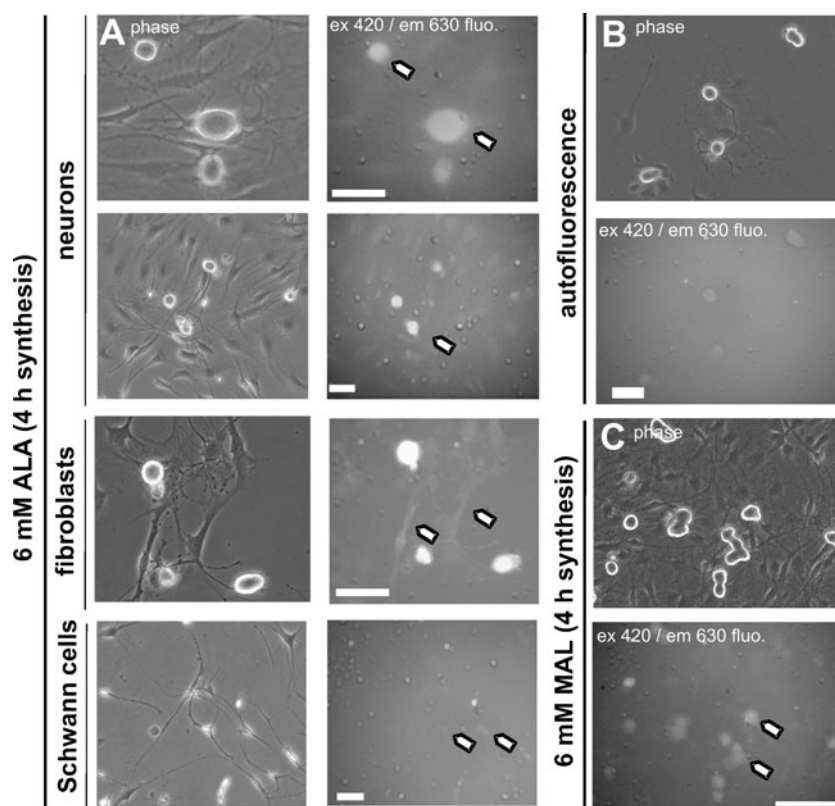
Comparable hyperbolic curve characteristics could be found when allowing ALA- or MAL-loaded cells to synthesize PpIX for 2 h after the 30 min uptake (Fig. 4c). Here, the maximum PpIX level, reached at an ALA concentration of 6 mM, was 2,105 RFU and nearly doubles with ALA concentrations increasing from 0.6 to 6 mM. With MAL, the highest fluorescence value of 1,787 RFU was seen at a concentration of 6 mM. Using MAL, the PpIX fluorescence for 0.6 mM was lower after 2 h than after 1 h incubation. The dose–response curve thus shows an inflection at 0.6 mM MAL for the 2-h incubation time. Prolonging the incubation time to 4 h (Fig. 4d), the dose–

response curve for ALA also shows a slight inflection at the lowest ALA concentration. No increase was seen in the fluorescence after 0.6 mM ALA and the 4-h compared to the 2-h incubation period. The curve also shows no saturation between 1.8 and 6 mM ALA, since the fluorescence still increases from 2,743 to 3,843 RFU. Prolonging the synthesis time to 4 h after MAL incubation results in a complete absence of PpIX fluorescence when using 0.6 mM MAL. With the higher MAL concentrations, fluorescence reached values of 600 and 2,483 RFU for 1.8 and 6 mM, respectively, yielding a curve with an almost linear appearance.

In total, the differences between ALA- and MAL-induced PpIX fluorescence after 30 min uptake were increasingly pronounced with longer synthesis times.

This is also sustained after 24 h of PpIX synthesis (Fig. 4e). At this interval, there is a strong reduction in the PpIX fluorescence values compared to the situation after

Fig. 2 Microscopic evidence for PpIX formation. PpIX-like fluorescence after synthesis from ALA (**a**) or MAL (**c**) was analysed using epifluorescence microscopy (greyscale pictures). Filters for 420 nm excitation and 630 nm emission were used. Untreated cell cultures (**b**) displayed only very weak autofluorescence at these wavelengths. Arrows in (**a**) indicate the particular cell type referred to on the left margin of (**a**). While cells with neuronal morphology display a markedly increased PpIX-like fluorescence after ALA treatment, this cannot be seen in cells with fibroblast or Schwann cell morphology. Arrows in (**c**) indicate neurones. Scale bars indicate 40 μ m



4 h. This is most pronounced for the low ALA and MAL concentrations, where there is virtually no fluorescence left in 0.6 mM ALA or MAL condition and also for the 1.8-mM condition, the fluorescence values decline towards the levels after 0 h synthesis time (287 and 79 RFU, respectively). Only the cells incubated with 6 mM ALA still show a pronounced PpIX fluorescence of 1,343 RFU after 24 h. This accounts for about a third of the PpIX fluorescence measured after 4 h synthesis. Such a long-sustained level could not be reported for the MAL-induced PpIX, where a residual 400 RFU remain from the maximal value of 2,483 RFU after 4 h.

To obtain EC_{50} values for pharmacological comparisons, the data from Fig. 4c were subjected to non-linear curve fits. The results are depicted in Fig. 5a. Performing a hyperbolic curve fit for the ALA dose–response after 30 min uptake and 2 h synthesis reveals an EC_{50} for the half-maximal PpIX formation of 0.734 ± 0.091 mM. The MAL dose–response requires fitting to a dose–response algorithm, where an EC_{50} for PpIX formation can be estimated at 1.641 ± 0.046 mM. The correlation coefficients were 0.998 and 0.996 for ALA and MAL, respectively. In relation to these results, the following experiments concerning the uptake mechanism were conducted with 0.6 mM ALA or 1.8 mM MAL (30 min uptake) at a synthesis time of 2 h (see Table 3).

Analysis of uptake pathways by competition and inhibition

As some amino acid transporters may be involved in ALA or MAL uptake (Rud et al. 2000; Gederaas et al. 2001), and the medium used for uptake (DMEM/F12 (1:1), Gibco) contained 20 biogenic amino acids, uptake in DMEM/F12 and a buffer free of amino acids (see Methods) was compared. The results are summarized in Fig. 5b. When applying 0.6 mM ALA in an amino acid free buffer, PpIX fluorescence increased by 498 RFU compared to ALA in culture medium. This represents a relative increase in PpIX fluorescence of 39.5%. This effect was statistically significant ($n=10$; $**p<0.01$; Mann–Whitney U test). A similar difference could not be observed with MAL, which elicits nearly the same amount of PpIX fluorescence in culture medium and in buffer (1,087 RFUs for culture medium, 1,019 RFUs for buffer). To identify amino acids that inhibit ALA-induced PpIX formation in DRG neurone cultures, 0.6 mM ALA was added to the cultures together with 15 different amino acids. Amino acids were used at a 10-fold higher concentration than in DMEM/F12 culture medium and were present throughout the 30 min uptake interval. The influence of amino acids on PpIX formation is presented in Fig. 5c. Some of the amino acids tend to reduce PpIX-like fluorescence after ALA incubation. This tendency is strongest seen with 7 mM L-arginine, 1 mM L-

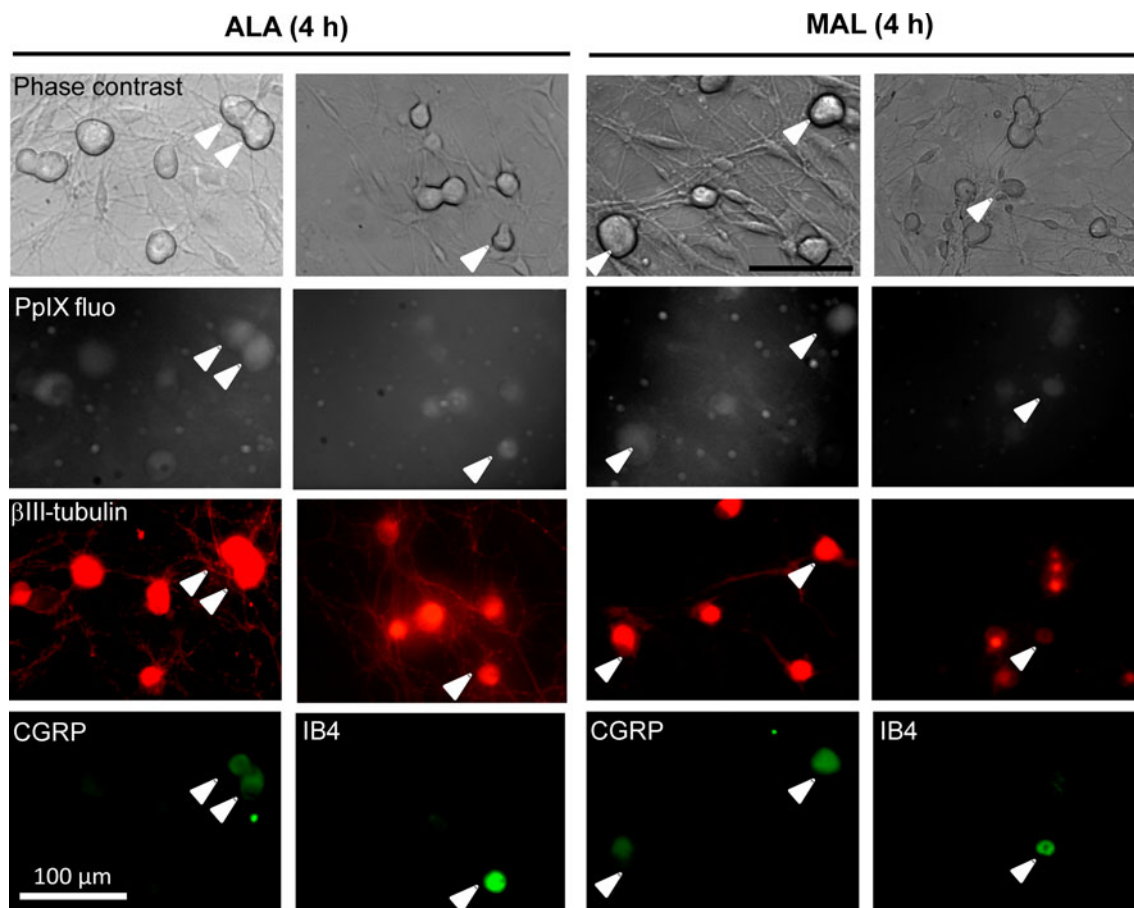


Fig. 3 Colocalisation of PpIX fluorescence with general neuronal and nociceptor subtype markers. PpIX-like fluorescence after synthesis from ALA or MAL was analysed using epifluorescence microscopy (greyscale pictures). Filters for 420 nm excitation and 630 nm emission were used. Phase contrast and corresponding PpIX-like fluorescence photomicrographs of live cells are depicted in the upper two rows. After this analysis, cell cultures were fixed and subjected to

β III-tubulin immunocytochemistry (red; row 3) in combination with either CGRP immunocytochemistry (green) or IB4 staining (green) (both row 4). Cells were relocated after the fixation and staining procedures using custom-made 500- μ m grids on the culture dish bottom. Examples for the colocalisation of ALA and MAL induced PpIX-like fluorescence with either CGRP or IB4 positive neurones are given and labelled with white arrowheads

methionine, 1 mM L-cysteine and 1.5 mM L-histidine. When microscopically analysing the cultures after the incubation, we observed atrophic cells in case of L-methionine and L-histidine and ALA co-incubation, which may have caused reduced PpIX signals in the cultures that were treated this way. Although none of the effects that were unrelated to toxicity proved statistically significant at first hand, a concentration–response experiment for L-arginine was carried out. The results are shown in Fig. 6a. L-arginine (L-Arg) was co-applied with either 0.6 mM ALA or 1.8 mM MAL in four concentration steps (1, 5, 10 and 20 mM) and PpIX fluorescence was read out. When co-incubating ALA and L-arginine, no decrease in PpIX fluorescence could be seen in the lowest L-Arg concentration, but with increasing L-Arg concentration, a significant reduction was visible. Fluorescence was reduced by 16% with 5 mM L-Arg, 28% with 10 mM L-Arg and 30% with 20 mM L-Arg, respectively. This difference was statistically significant in a Mann–Whitney *U*

test ($n=3$; $*p<0.05$). Interestingly, when co-incubating L-Arg with MAL, for which no influence was seen in Fig. 5b, there was also a reduction in PpIX-fluorescence. Although only statistically significant ($n=3$; $*p<0.05$) for 10 mM L-Arg (33% reduction), a tendency of reducing PpIX fluorescence is seen throughout all three L-Arg concentrations above 1 mM.

BETA transporters, usually involved in the uptake of γ -aminobutyric acid (GABA) and structurally related compounds have been strongly implicated in ALA uptake but discussed as less relevant for MAL uptake (Bermudez et al. 2002; Rodriguez et al. 2006). We applied different BETA transporter substrates or blockers to characterize the role of these membrane proteins in ALA and MAL uptake. The results are summarized in Fig. 6b. Co-application of 0.6 mM ALA or 1.8 mM MAL with 10 mM GABA led to a decrease in PpIX fluorescence induced by both pro-drugs. GABA reduced ALA induced fluorescence by 35% and MAL induced fluorescence by 34%. β -alanine, which has higher

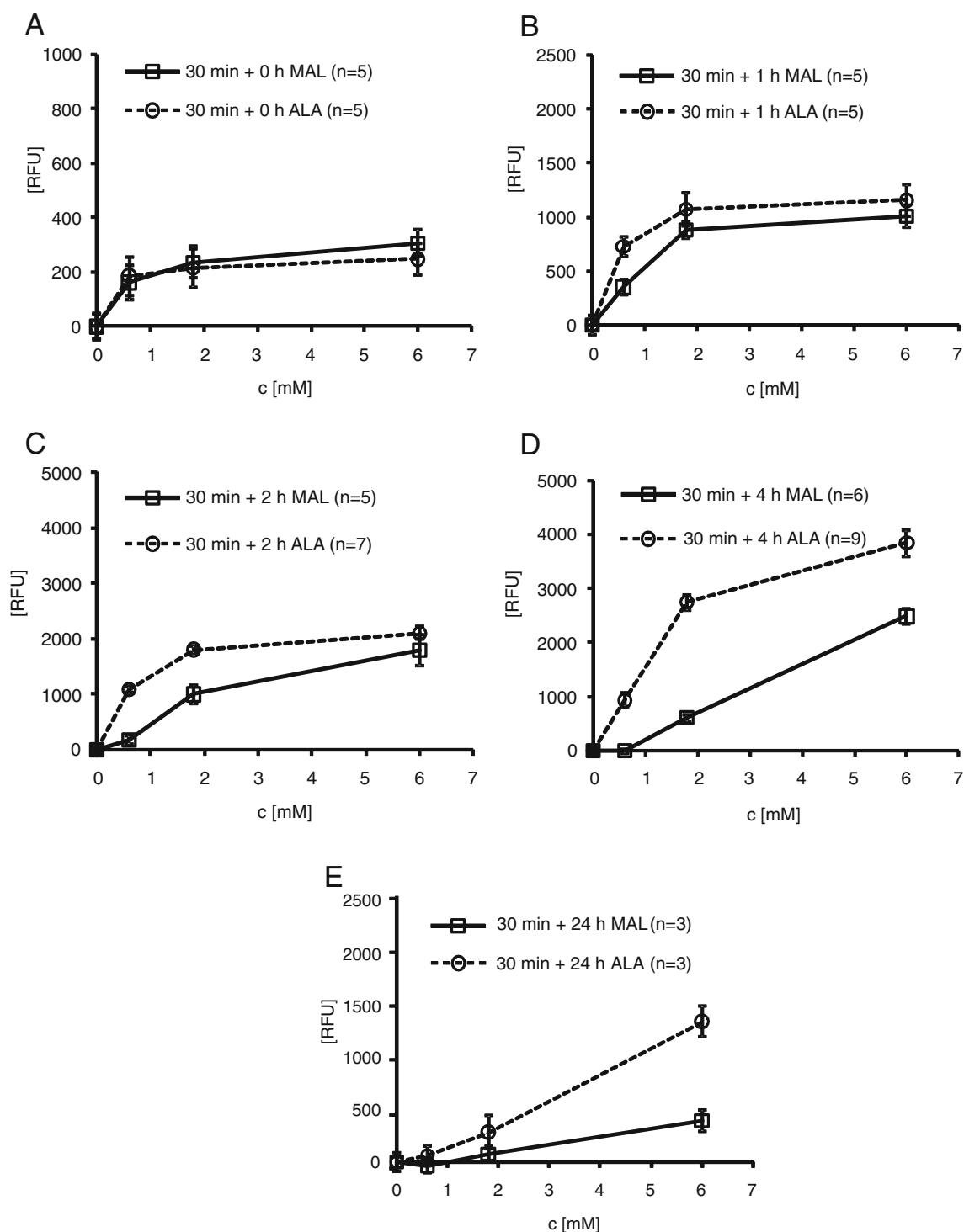


Fig. 4 Formation of PpIX in DRG neurone cultures after incubation with ALA or MAL. Cells from the DRG were cultured for 48 h in microtitre plates before being subjected to ALA or MAL incubation. Both pro-drugs were dissolved in DMEM/F12 culture medium with NGF at pH 7.4. Graphs compare the PpIX formation after 30 min ALA or MAL uptake, followed by synthesis intervals of 0 h (a), 1 h (b), 2 h (c), 4 h (d), 24 h (e). In order to terminate uptake after 30 min, cultures were washed with

fresh medium. After the indicated synthesis times, cells were lysed and PpIX fluorescence was assessed. This fluorescence is indicated in relative fluorescence units measured at 390 nm excitation and 620 nm emission. Note that the axis intercept is chosen differently in order to facilitate the interpretation. Data points represent the mean values from five to nine independent experiments (see graph for details). Error bars represent standard errors of the mean (SEM)

selectivity for GAT-2, also reduced ALA- and MAL-derived PpIX by 40% and 28%, respectively. β -Alanine thereby

prove more effective in competitively inhibiting ALA uptake. The compounds guvacine and (*S*)-SNAP 5114 block

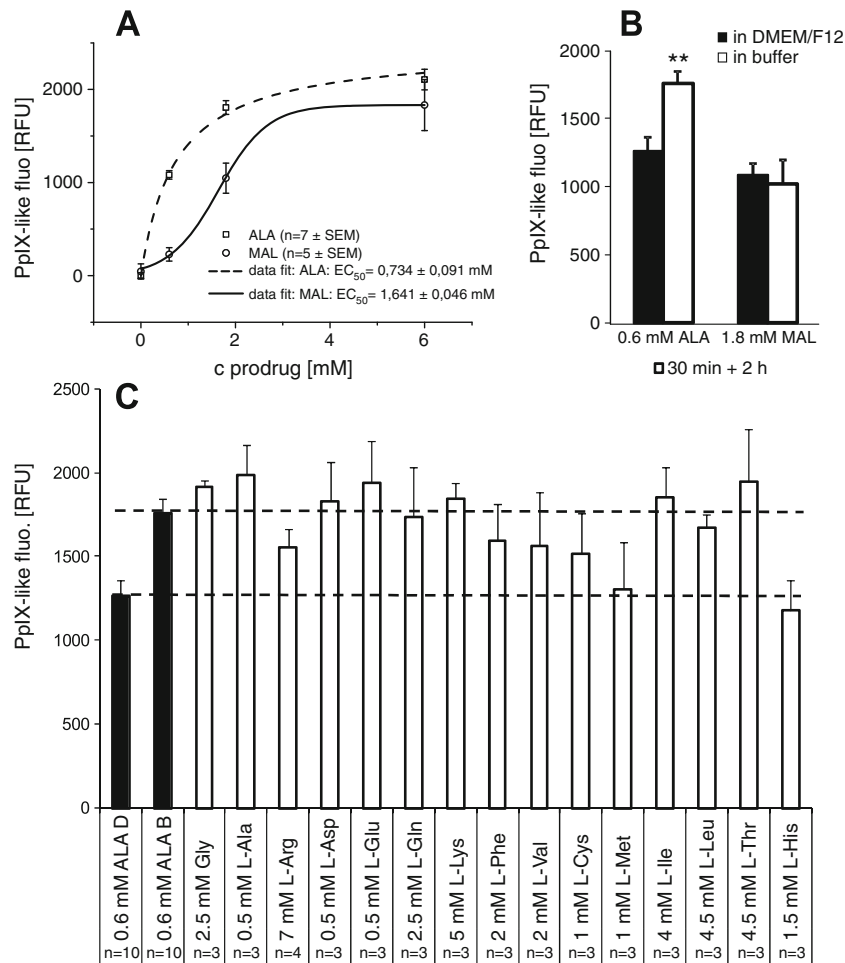


Fig. 5 Non-linear fits for PpIX formation from ALA and MAL after 2 h synthesis time and influence of culture medium and amino acids on PpIX formation. **a** DRG neurone cultures were treated with different concentrations of ALA and MAL for 30 min, washed and allowed to synthesize PpIX for 2 h. Cells were then lysed and PpIX-like fluorescence (390 nm excitation and 620 nm emission fluorescence) was quantified. Pro-drugs were dissolved in DMEM/F12 or HEPES buffer. EC₅₀ values were estimated using a hyperbolic fit algorithm for ALA and a dose–response–algorithm for MAL. ALA displays an EC₅₀ of 0.734±0.091 mM, MAL of 1.641±0.046 mM. **b** By both dissolving ALA (0.6 mM) and MAL (1.8 mM) either in DMEM/F12 or a HEPES buffer, the influence of medium components on PpIX was analysed.

Cells were incubated and analysed as in (a). Dissolving ALA in buffer results in an absolute increase in PpIX formation by 498 RFU, which represents a relative increase of 39.5%. This effect cannot be observed with 1.8 mM MAL. (n=10 for ALA in DMEM/F12 or buffer, and for MAL in DMEM/F12; n=6 for MAL in buffer. Error bars represent SEM. **P<0.01; Mann–Whitney U test). **c** DRG neurone cultures were co-incubated with 0.6 mM ALA and various amino acids, always at a 10-fold higher concentration than present in DMEM. Compounds were dissolved in the buffer used in (b). Cells were otherwise processed as in a and b. Some amino acids (L-methionine, L-histidine and L-arginine) cause a reduction in PpIX formation

Table 3 Summary of pharmacological properties of ALA- and MAL-induced PpIX induction and inhibitory potential of GABA transporter blockers

Pro-drug	inhibitor	EC ₅₀ ^a	IC ₅₀ ^a	Std.-Error	K _i ^b	Std. Error	pK _i ^b
ALA		0.734 mM		±0.091			
MAL		1.641 mM		±0.046			
ALA	vs. guvacine		4.620 mM	±1.210 mM	2.45 mM	±0.54 mM	2.61
	vs. (S)-SNAP 5114		0.355 mM	±0.01083 mM	195 μM	±6 μM	3.71
MAL	vs. guvacine		3.390 mM	±0.684 mM	1.62 mM	±0.33 mM	2.79
	vs. (S)-SNAP 5114		0.270 mM	±0.7775 mM	129 μM	±13 μM	3.89

^a 30 min uptake and 2 h synthesis

^b From Cheng-Prusoff equation

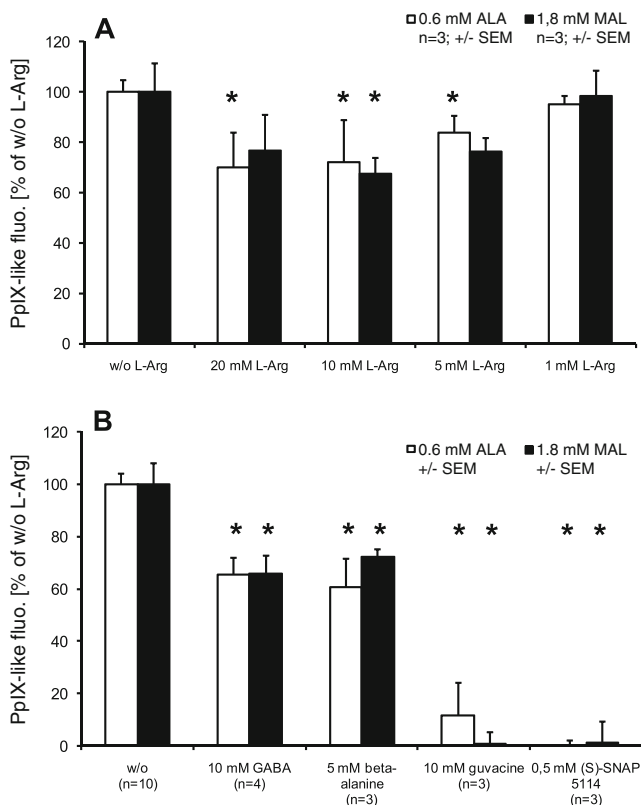


Fig. 6 Influence of L-arginine and GABA on PpIX formation in DRG neurone cultures after extracellular application of ALA or MAL. Cells from the DRG were cultured for 48 h in microtiter plates before being subjected to ALA or MAL incubation. Both pro-drugs were dissolved in a physiological HEPES buffer of pH 7.4 containing NGF and then co-applied with either L-arginine (a) or GABA-related compounds (b). In order to terminate ALA- or MAL-induced uptake after 30 min, cultures were washed with fresh medium. After 2 h of additional synthesis time, cells were lysed and PpIX-like fluorescence was assessed. Graphs compare the PpIX formation from 0.6 mM ALA (white bars) and 1.8 mM MAL (black bars) alone or after co-incubation with either different concentrations of L-Arg (1–20 mM) or 10 mM GABA, 5 mM β -alanine, 10 mM guvaccine or 0.5 mM (S)-SNAP 5114. Relative PpIX formation is given as percent of PpIX formation without inhibition. A relative reduction of ALA-induced PpIX-like fluorescence by 30% was reached by the maximal L-Arg dose (20 mM) applied. The lower doses of 10 and 5 mM reduced PpIX-like fluorescence by 28% and 16%, respectively. These effects prove statistically significant in the Mann–Whitney *U* test ($*p < 0.05$). MAL-induced PpIX-like fluorescence is also reduced by L-Arg co-incubation. The maximal reduction is reached after co-incubation with 10 mM L-Arg (33%). Co-incubation with the lower concentrations of L-Arg is less effective (23% reduction by 20 mM and 24% reduction by 5 mM L-Arg, respectively). These two effects were proven to be not statistically significant (Mann–Whitney *U* test, $p < 0.05$). When co-incubating ALA and MAL with 10 mM GABA, a reduction by 35% and 34% is measured, respectively. Co-incubation of the pro-drugs with 5 mM β -alanine reduces the PpIX-like fluorescence by 40% in case of ALA and by 28% in case of MAL. The GAT-1 blocker guvaccine at a concentration of 10 mM reduced PpIX production to 12% with ALA and to 1% with MAL. The GAT-2/3 blocker (S)-SNAP 5114 (0.5 mM) reduced ALA and MAL induced PpIX to 0 or 1%, respectively. All the reported results were statistically significant in the Mann–Whitney *U* test with $p < 0.05$. Data points represent the mean values of independent experiments (compare graph for details). Error bars represent standard errors of the mean (SEM)

GABA transporters. While guvaccine strongly favours blocking GAT-1, (S)-SNAP 5114 is GAT-2 and GAT-3 selective. Both blockers strongly reduced PpIX formation from ALA and MAL in DRG neurone cultures. Only 12% of the control level of PpIX remained, when ALA and 10 mM guvaccine are co-applied. MAL induced PpIX was reduced to 1%. (S)-SNAP 5114 was even more effective, as it virtually abolished ALA or MAL derived PpIX formation in DRG neurone cultures at a concentration of 0.5 mM. In summary, GABA transporter inhibitors at high concentrations are able to nearly completely inhibit PpIX production from ALA and MAL.

To analyse whether the reductions in PpIX formation by L-arginine (as seen in Fig. 6a) and by GABA transporter substrates (Fig. 6b) are additive, we applied 0.6 mM ALA together with 5 mM β -alanine and 20 mM L-Arg. The result is depicted in Fig. 7a. While β -alanine and L-Arg alone displayed the expected effects of reducing PpIX at a similar amount, the combination of both substances failed to trigger a significantly increased inhibition. PpIX formation was reduced further by 10%, but this was not statistically different to the effects of the substances alone. Both substances and their combination reduced fluorescence significantly when compared to the control level ($n=4$; $*p < 0.05$; Mann–Whitney *U* test). Thus, no clear additive effect could be described here.

To more accurately determine the pharmacology of GAT-related membrane transport of ALA and MAL, concentration–response measurements were performed. ALA (0.6 mM) and MAL (1.8 mM) were co-incubated with increasing concentrations of guvaccine (10 μ M to 10 mM) and (S)-SNAP 5114 (10 μ M to 0.5 mM). The results are displayed in Fig. 8a–d. The blockers greatly reduced ALA and MAL uptake and thereby PpIX formation in a concentration-dependent manner.

In order to compare the pharmacological parameters of uptake inhibition by guvaccine and (S)-SNAP 5114 between ALA and MAL, the datasets from Fig. 8a–d were subjected to non-linear fits. The results are presented in Fig. 8e, f.

Figure 8e illustrates the concentration–response relationships between ALA and MAL co-incubated with guvaccine. A Hill-Fit equation was used to determine IC_{50} values as a measure for half-maximal inhibition of PpIX formation. The two curves resulting from both datasets displayed similar characteristics. IC_{50} values and the calculated K_i and pK_i values for guvaccine are summarized in Table 3. The K_i and pK_i values were calculated using the Cheng-Prusoff equation employing the EC_{50} values for ALA/MAL determined in Fig. 5a (see Methods).

Figure 8f shows Hill-Fits of the concentration–response curves for (S)-SNAP 5114 blocking either ALA or MAL induced PpIX formation. Like in Fig. 8e, the curves displayed considerable similarities in their characteristics. IC_{50} and pK_i values for ALA and MAL versus (S)-SNAP 5114 are presented in Table 3.

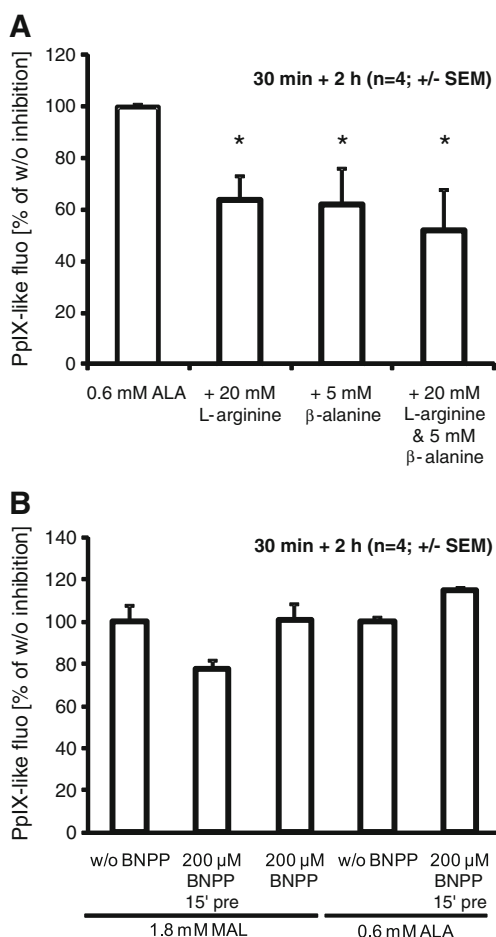


Fig. 7 Additive effect of GABA and L-arginine on PpIX inhibition and contribution of extracellular esterases. **a** To assess whether β-alanine- and L-arginine-induced inhibition of ALA-derived PpIX requires different uptake mechanisms, the two substances were co-incubated with 0.6 mM ALA in their maximal effective concentration (**a**). β-alanine alone (5 mM) reduced PpIX formation to 62%, while L-arginine (20 mM) alone reduced PpIX to 64%. Co-incubation of the cells with both substances reduced PpIX formation to 52%. All effects are statistically significant (Mann–Whitney *U* test; **p*<0.05) compared to the control (ALA without block), but no significance occurs between the individual compounds and their combination. **b** In order to clarify whether the methyl-ester group of MAL is cleaved by extracellular carboxyesterases, MAL (and ALA as control) was applied to cells pre-treated with the carboxyesterase inhibitor BNPP (200 μM). When BNPP was added to the cultures 15 min prior to the addition of MAL (1.8 mM), PpIX formation is reduced by 23%. This effect is absent, when no pre-incubation is carried out and 200 μM BNPP is added simultaneously to 1.8 mM MAL incubation. Cells pretreated with 200 μM BNPP and subjected to 0.6 mM ALA increase the amount of PpIX formed by 15%

Influence of extracellular esterases on MAL uptake

The experiments conducted until here were suggestive of a very similar uptake pathway for ALA and MAL into cultured DRG neurones. Disabling the activity of extracellular carboxyesterases present on or secreted by the cells in our test system may give evidence on the fact whether

MAL could be converted to ALA before crossing the cell membrane. The membrane impermeable carboxyesterase inhibitor BNPP was therefore added to the cells either immediately or 15 min before adding 1.8 mM MAL and stayed present during the uptake period (Fig. 7b). When 200 μM BNPP were added 15 min prior to MAL addition, a reduction by 23% in PpIX fluorescence by 23% could be observed. This effect was absent when BNPP was added directly together with MAL and stayed present for the uptake period only. As a control experiment, cells to be subjected to 0.6 mM ALA uptake were also pre-treated for 15 min with 200 μM BNPP. Here, no decrease—but rather an increase by 15%—in PpIX formation could be seen. Results were tested for statistical significance (*n*=4; **p*<0.05; Mann–Whitney *U* test).

Expression of GABA transporter mRNA in rat DRG cultures

For mRNA expression analysis, cDNA was synthesised from RNA isolated from neocortex, liver and cultured DRGs. Neocortex served as a positive control for GAT-1 and GAT-3 (Vitellaro-Zuccarello et al. 2003), while liver served as a positive control for GAT-2 (Liu et al. 1999). RT-PCR results are depicted in Fig. 9a. The first four lanes after the size standard represent the positive controls for GAT-1 and GAT-3. Bands were clearly visible in the +RT condition and absent when reverse transcriptase had been omitted during cDNA synthesis. Lanes 5 and 6 show the positive control for GAT-2 with cDNA from rat liver. All bands appeared at the expected positions relative to the size standard. Analysing cDNA from cultured rat postnatal day 3 (P3) DRGs, clearly revealed the expression of GAT-1 (lanes 7 and 8) and GAT-3 (lanes 11 and 12), with a PCR product only in the +RT condition, while mRNA for GAT-2 (lanes 9 and 10) was clearly absent in cultured DRG neurones.

As an additional means of validation for GAT expression in sensory neuron cultures, uptake of [³H]-labelled GABA was conducted. Figure 9b shows uptake of GABA into neuronal cultures, which can be clearly reduced by increasing the proportion of unlabelled GABA. Addition of 1 mM unlabelled GABA to the 0.1 mM of labelled GABA results in a reduction of uptake to 44% of the control value, while a further increase of unlabelled GABA to 10 mM fully abrogates [³H]-GABA incorporation. Blocking the uptake of 0.1 mM [³H]-labelled GABA with the GAT-3 selective blocker (*S*)-SNAP 5114 at a concentration as low as 0.1 mM leads to a reduction of [³H]-GABA to 21% of the control value (without inhibition). Reducing the concentration of (*S*)-SNAP 5114 to 50 μM diminishes inhibition to a remaining uptake of 42%. The reductions seen with both GABA concentrations and with 100 μM (*S*)-SNAP 5114 were

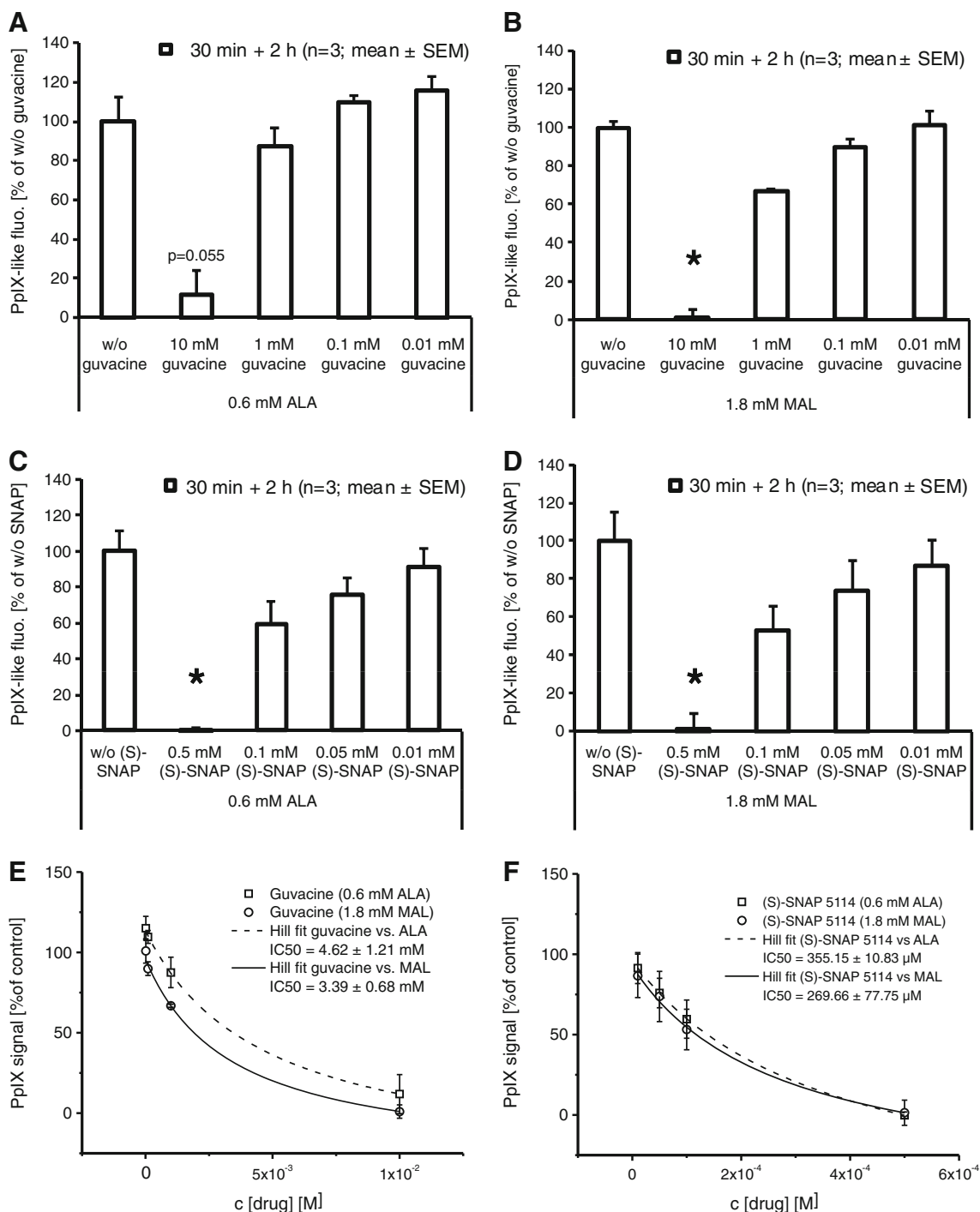


Fig. 8 Concentration–response experiments for the GABA transporter blockers guvaccine and (S)-SNAP 5114. DRG neurone cultures were co-incubated with 0.6 mM ALA (**a, c**) or 1.8 mM MAL (**b, d**) and the blockers guvaccine (GAT-1 selective) and (S)-SNAP 5114 (GAT-2/3 selective). The experimental procedure was identical to the one described for Fig. 5. Increasing concentrations of both blockers could reduce the PpIX formation from both ALA and MAL. Application of (S)-SNAP 5114 led to complete inhibition of PpIX formation at low drug concentrations. Synthesis times were always 2 h. Columns represent mean value of three independent repeats \pm SEM. * $p \leq 0.05$; ANOVA on ranks with Dunn's post-test. The inhibition of PpIX formation from ALA or MAL is plotted as inhibition curves in **e** and **f**.

Data points represent mean values of $n=3$ independent experiments with error bars representing SEM. Inhibitory capacity of guvaccine against 0.6 mM ALA (solid line) or 1.8 mM MAL (dotted line) are shown in **e**, while inhibitory capacity for (S)-SNAP 5114 is shown in **f**. Data were fit to Hill equations to determine half-maximal inhibitory effect (IC_{50}). Correlation coefficient (r^2) values are 0.99846/0.99999 (ALA guvaccine/SNAP) and 0.99207/0.99581 (MAL guvaccine/SNAP). The IC_{50} of guvaccine was 4.62 ± 1.21 mM for inhibition of ALA induced PpIX and 3.39 ± 0.68 mM for inhibition of MAL-induced PpIX. For (S)-SNAP 5114, IC_{50} values of 355.15 ± 10.83 μ M (ALA) and 269.66 ± 77.75 μ M (MAL) were calculated from the fits

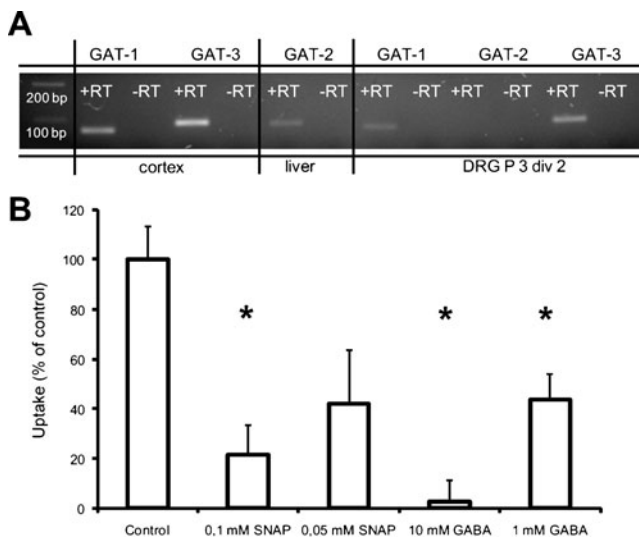


Fig. 9 Expression of GABA transporter subtypes in the test system. Picture of an ethidium bromide stained agarose gelelectrophoresis separating the products of an RT-PCR with intron-spanning primers designed to amplify rat GAT-1, GAT-2 or GAT-3 from cDNA (**a**). Postnatal rat cortex cDNA was used as positive control for GAT-1 and 3 expression, while liver cDNA from postnatal rats was used as GAT-2 positive control. PCR products were expected to have the sizes 166 (GAT-1), 185 (GAT-2) and 191 (GAT-3). –RT indicates the controls, were no reverse transcriptase was added in cDNA synthesis, while +RT indicates samples with reverse transcriptase added in cDNA synthesis. The DNA ladder runs in the *leftmost lane* and displays the 100 and 200 bp bands. The *next four lanes* depict positive GAT-1 and GAT-3 expression in cortex tissue. GAT-2 is expressed in postnatal rat liver cDNA (*lanes 6 and 7*), while in DRG neurones cultivated for 2 days only the expression of GAT-1 and GAT-3 was confirmed (*lanes 8–12*). Uptake of [³H]-radiolabelled GABA into sensory neuron cultures is depicted in **B**. Sensory neurones were cultured in 96-well-plates for 48 h before being incubated with [³H]-GABA in presence or absence (control) of inhibitors. *Columns* indicate the relative incorporation of radioactively labelled GABA (0.1 mM; 0.064 MBq/ml) referring to the control condition without inhibition. Inhibition of uptake was achieved either by an excess (1 or 10 mM) of unlabelled GABA or by the GAT-3 specific inhibitor (S)-SNAP 5114 at concentrations of 0.05 or 0.1 mM. Both concentrations of unlabelled GABA and the 0.1 mM concentration of (S)-SNAP 5114 were capable of significantly reducing the uptake (Mann–Whitney *U* test; * $p \leq 0.05$; $n=4$). *Error bars* show the standard error of mean (SEM)

proven statistically significant using the Mann–Whitney *U* test ($n=4$; * $p < 0.05$).

Neurotoxicity of ALA and MAL in a morphometric assay

To investigate potential neurotoxic effects of ALA and MAL on the neuronal cultures, a morphometric assay for neurite degeneration was conducted. The results are depicted in Fig. 10; 6 mM ALA or MAL were added to the neurones; uptake was allowed for 30 min. The synthesis intervals were 2 and 4 h, as these conditions yield the maximum PpIX productions from the pro-drugs and are thus mostly prone to toxic effects. The exemplary pictures

in Fig. 10a show the neuritic networks in cultures treated to the abovementioned effect. Here, no impairment of the network can be seen at first sight. An elaborate investigation measuring the longest neurite of each neurone present in the samples (Fig. 10b) also revealed no significant reduction in neurite length (Mann–Whitney *U* test; * $p \leq 0.05$; $n=3$). The neurite length is expressed as percent relative to an untreated control kept under standard culturing condition and always processed in parallel to the experimental conditions to rule out influences of culturing and staining variance. Thus, using this assay, no influence of ALA or MAL incubation and PpIX formation on the viability of the cultures could be detected. Additionally, no reduction in total neurone numbers were seen when evaluating cells cultures for this assay, ruling out cellular loss by cell death processes.

Discussion

While being an undoubtedly effective treatment for cutaneous malignancies, ALA- and MAL-PDT bear one major drawback: the pain experienced during the illumination phase (Grapengiesser et al. 2002; Ericson et al. 2004; Kasche et al. 2006; Lindeburg et al. 2007). Two different pathways for pain generation can be envisaged, both involving sensory neurone activation. While algogenic messengers may be released from PDT-treated tissue, it is also conceivable that photodynamic action occurs directly in sensory fibres in the skin. An inevitable imperative for this possibility is the generation of PpIX in sensory neurones. In the current study, we chose a cell culture test system to gather information on the ability of cultured sensory neurones to generate intracellular PpIX from externally applied ALA and MAL. The advantages of this *in vitro* approach are full control of the experimental parameters and direct accessibility of the peripheral neurones. The disadvantage, however, is the fact that in the clinical situation only the intraepidermal processes of the sensory neurones are subjected to PDT. However, the use of cultured sensory neurones is common practice in nociception research and results gathered here are widely agreed to be transferrable to more naturalistic scenarios (e.g. Vyklicky and Knotkova-Urbancova 1996; Passmore 2005). Of the different sensory neurone subtypes, C-fibre neurones are most likely to extend processes into epidermal layers (Lumpkin and Caterina 2007). To underline the validity of our test systems, the presence of the two principle kinds of C-fibre neurones (CGRP positive and IB4 positive) (Stucky and Lewin 1999; Priestley et al. 2002) was investigated. We could identify both subtypes of nociceptive, epidermis-associated C-type neurones in our culture system (Fig. 1). Thus, the *in vitro* test system contains the relevant neurone subtypes at a quantity that at least for CGRP (32%) resembles the proportions reported from the ganglion in

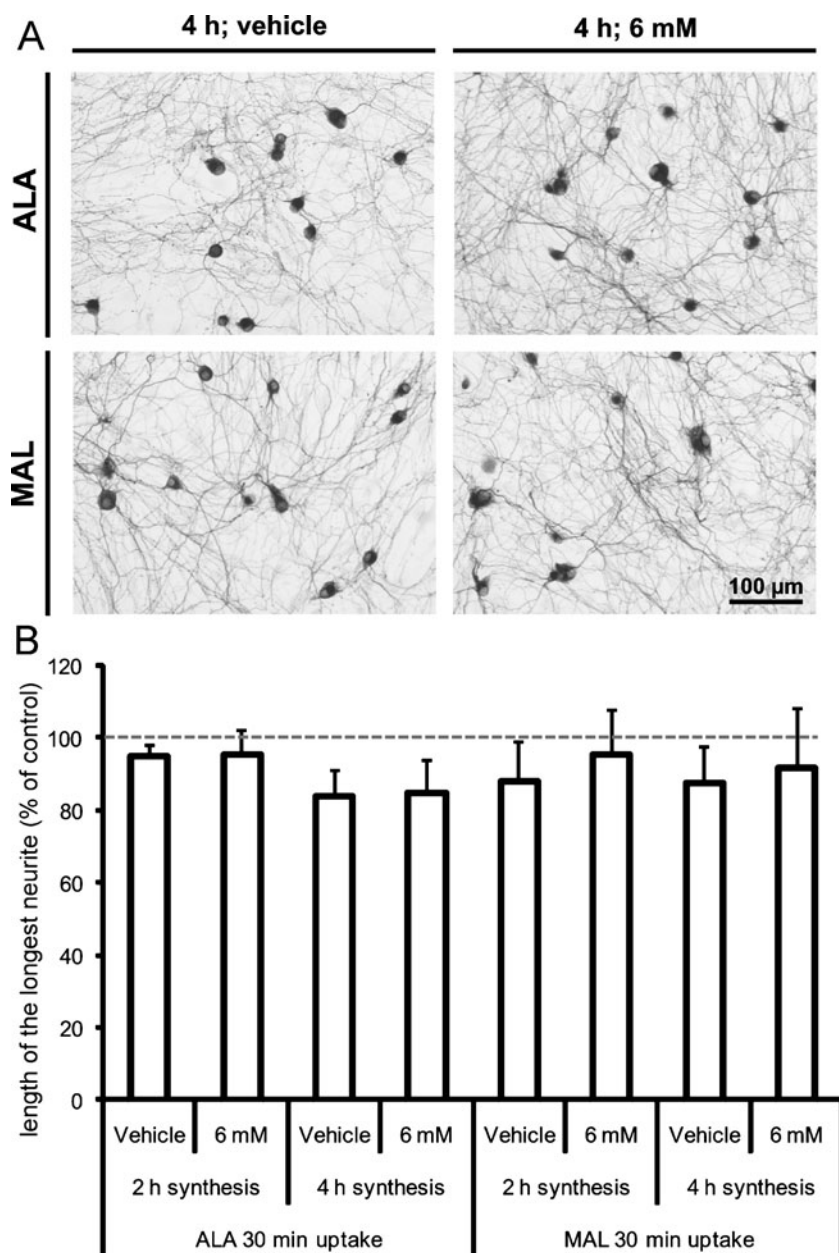


Fig. 10 Assessment of neurotoxicity using a morphometric assay. Sensory neurone cultures at 48 h *in vitro* were incubated with 6 mM ALA or MAL for 30 min, while PpIX synthesis was conducted for 2 or 4 h. Cultures were then fixed and stained using β III-tubulin immunocytochemistry. Experiments were carried out as three independent repeats, with three pictures taken from each culture dish at random positions. The longest neurite of all sampled neurons was measured using ImageJ software. The pictures under **a** are representative of the neuronal networks visible after 4 h PpIX synthesis from 6 mM ALA or MAL

and the corresponding vehicle controls. The quantification under **b** relates the measured neurite lengths to control cultures cultivated under standard conditions and always analysed in parallel to all three independent repeats. The mean length of the longest neurites found in these cultures is set as 100% (dashed grey line in **b**). The columns represent the mean relative length of the longest neurite under the different experimental conditions, *error bars* show the standard error of mean (SEM). No significant reductions in the length of the neurites could be found using the Mann–Whitney *U* test ($p \leq 0.05$; $n=3$)

vivo (Priestley et al. 2002). The relatively low yield in IB4+ neurones can be explained by their greater dependence of GDNF as a neurotrophic factor (Lumpkin and Caterina 2007). In total, almost half the neurones in the culture system used for these studies display markers characteristic of nociceptors.

In a heterogeneous culture system as ours, assessment of PpIX fluorescence at the single cell level should clarify, whether PpIX fluorescence can be elicited in the neuronal fraction. A custom-built epifluorescence filter set (420 nm excitation; 630 nm emission with a 470 nm beam splitter) allowed to visualize PpIX microscopically. In our experi-

ments, neuronal cells (as identified by their unique morphology) responded to ALA or MAL incubation with the greatest increase in PpIX. A fluorescence increase of similar intensity was absent in the other two morphologically distinct cell types (Schwann cells and fibroblasts). Many steps of the conversion of ALA to PpIX take place intramitochondrially. Neurones are, due to their high-energy requirement, equipped with a massive mitochondrial network. On the other hand, due to their spherical appearance, one might overestimate the PpIX fluorescence when comparing neurones to flat cells with a more planar extension such as fibroblasts. Nevertheless, the massive predominance of neuronally localized PpIX-fluorescence in the cultures intrigued us to draw the conclusion that PpIX fluorescence in DRG neurone cultures is mostly due to neurones, such that the PpIX measured in cell lysates from such cultures allows the assessment of the formation of PpIX in neurones. Staining of cells beforehand assayed for PpIX production with an antibody against β III-tubulin could furthermore clearly verify the neuronal identity of neuronally shaped PpIX-producing cells. Using double stains with anti- β III-tubulin antibodies and anti-CGRP antibodies or isolectin B4, respectively, it could also be shown that the potentially nociceptive fraction of neurons in the cultures contributes to the PpIX formation. This greatly supports the notion that PpIX is produced directly in pain-related neuronal structures. It thereby contributes to the pain experienced in ALA and MAL PDT, as both pro-drugs trigger PpIX production in nociceptors alike.

Quantification of PpIX derived from ALA or MAL shows that PpIX formation in sensory neurones is a function of pro-drug concentration and synthesis time. Our experiments combined a distinct uptake step (30 min) with varying synthesis times. This ensures that always a constant amount of pro-drug is provided for the PpIX synthesis machinery. It can be clearly derived from the graphs in Fig. 3, that the differences between ALA- and MAL-induced PpIX increase with prolonged synthesis time. Two explanations may account for this: (1) different amounts of ALA and MAL are taken up during the 30 min time window. If this amount was lower for MAL (as suggested by Washbrook et al. 1997; Uehlinger et al. 2000) the decrease in PpIX after low MAL concentrations and prolonged synthesis times could be due to pro-drug depletion and an overweight in the conversion of PpIX to heme and subsequent breakdown. (2) The additional hydrolysis step converting MAL to ALA is rate-limiting. This would lead to a lag in PpIX build-up and also promote breakdown. Three facts argue in favour of hypothesis one. First, the highest MAL concentration (6 mM) does not show a time-dependent decline but provides a constant increase in PpIX over time. This is also the fact for the lower ALA concentrations (1.8 mM). Second, Kloek et al.

(1998) concluded from their studies in Jurkat cell lysates that the hydrolysis step for MAL insignificantly alters PpIX formation. And third, when PpIX fluorescence is measured immediately after the uptake, levels for ALA and MAL are nearly identical. This would not be possible, if MAL had to undergo a rate-limiting, time-consuming hydrolysis step. Even after a 24-h synthesis interval, MAL-derived PpIX is still present in the cell cultures, when 6 mM pro-drugs were applied. This is also the fact in ALA-treated cultures, although the remaining PpIX amount is clearly higher after 24 h. The long persistence of PpIX fluorescence seems thus related to the maximally synthesised amount, which suggest that PpIX breakdown is not a significant parameter after short synthesis intervals. As our experiments also support the notion, that the maximal PpIX amount is dependent on the amount taken up in the first place, any differences observed in PpIX production here are likely to be attributed to differences in ALA and MAL uptake efficiency.

Taken together these arguments are suggestive of a reduced uptake of MAL, which is in line with the reduced MAL uptake and MAL-induced PpIX formation described in a plethora of other cell culture systems (Gaulhier et al. 1997; Tunstall et al. 2002; Rodriguez et al. 2006; Lee et al. 2008).

The analysis of EC_{50} values of PpIX formation after 2 h synthesis further corroborates our finding, as the EC_{50} for MAL is higher by a factor of more than 2 than that for ALA (1.641 mM for MAL vs. 0.734 mM for ALA).

Neurotoxicity can represent a serious problem when working with ALA and PpIX (Riopelle and Kennedy 1982). We have thus assessed potential neurotoxicity of ALA and MAL using a neurite outgrowth/degeneration assay that already proves to be very sensitive towards subtle changes in neuronal viability (Schmidt et al. 2011). Experimental conditions were chosen in order to subject the neurones to maximal ALA and MAL levels (6 mM for 30 min) and to synthesize intervals yielding the maximal PpIX amount (2 and 4 h). As we could detect an influence neither of ALA or MAL concentrations nor of the synthesis conditions on the length of the neuronal neurites, a neurotoxicity can clearly be doubted. In addition, none of the cultures showed evident neuronal loss, so that cell death can most probably be neglected here.

Rud et al. suggested in 2000 that amino acids influence ALA uptake. We therefore substituted culture medium (DMEM/F12 1:1) with the buffer suggested in the above-mentioned study. An increase in ALA-derived PpIX could be observed, while this was not the case for MAL. This suggests either an influence of the amino acids in the medium on ALA transport or a slightly different Na^+ content in medium and buffer (ca. 136 vs. 150 mM Na^+). While ALA uptake is sensitive to Na^+ at this concentration range, MAL uptake is rather robust towards this parameter (compare Rud et al. 2000 and Gederaas et al. 2001). This

might explain the increase in ALA but not MAL seen in Fig. 4b. In order to further investigate whether amino acids alter neuronal ALA uptake, we performed the ALA uptake in buffer and in the presence of one of 15 different amino acids. The amino acids L-arginine, L-histidine and L-methionine altered ALA derived PpIX when applied at ten-fold higher concentrations than in DMEM/F12. As L-methionine- and L-histidine-treated cultures displayed signs of severe atrophy, we only continued with L-Arg. We observed a significant reduction in both ALA- and MAL-induced PpIX formation at high L-Arg concentrations. Our prior finding that MAL uptake was unaffected by amino acids in DMEM/F 12 may be explained by the L-Arg concentration in this medium, which is only 0.699 mM. The maximal inhibition achieved by high concentrations of L-Arg was 30%. The inhibition may be due to systems B^{0,+} and y^{+L} (SLC6A14 and SLC7A6 and SLC7A7, respectively, for Na⁺-dependent transport; Hyde et al. 2003), which are responsible for L-Arg translocation and have previously been suggested as carriers in ALA uptake (Rud et al. 2000).

Rud et al. (2000) had also found that ALA uptake in WiDr adenocarcinoma cells is dependent on GAT, while follow-up study by the same group a year later did not find MAL uptake through these transporters (Gederaas et al. 2001). This difference in uptake has led authors to the hypothetical assumption that ALA, but not MAL, would enter sensory neurones, as the GAT subtypes would be preferentially expressed in such neuronal cells. Following our evidence that MAL is also taken up by neurones, we investigated the GAT dependence of neuronal ALA/MAL uptake.

Four different competing substrates and blockers were applied in order to block ALA/MAL derived PpIX formation in DRG cultures. All of them showed some significant effect. Interestingly, their ability to prevent PpIX formation was nearly indistinguishable, when PpIX formation was stimulated by ALA or MAL close to their respective EC₅₀ values (0.6 mM ALA; 1.8 mM MAL). This suggests that both compounds share an entrance pathway into DRG neurones. While the competitive inhibition by co-substrates (GABA and β -ala) never exceeds 40%, PpIX signals can fully be blocked by guvacine (GAT-1 selective blocker) and (S)-SNAP 5114 (GAT-2/3 selective blocker). Notably, (S)-SNAP 5114 fully blocked PpIX formation at a 20-fold lower concentration than guvacine. The 10-fold higher ability of (S)-SNAP 5114 to block uptake as compared to guvacine strongly favours a GAT-2/3-mediated mechanism. Guvacine, at this high concentration (10 mM) would, according to its pharmacology (Borden 1996 and Kragler et al. 2005), lose its selectivity for GAT-1 and also block GAT-2 and 3. As no expression studies for GABA transporters in DRG, either in vivo or in vitro, could be found in sufficient detail, we performed an RT-PCR to analyse expression in our cultures. We could show a clear and robust expression of GAT-1 and

GAT-3 but not GAT-2. This suggests the involvement of GAT-3 in the uptake into sensory neurones. A further validation of the importance of GAT-3 for GABA (and thereby probably also ALA and MAL) uptake, comes from the studies using radiolabelled GABA. Here, it could clearly be shown, that (S)-SNAP 5114 is capable of reducing 0.1 mM GABA uptake at a concentration as low as 0.1 mM to a remaining extend of 21%. Further increases in (S)-SNAP 5114 could not significantly reduce the uptake of GABA any further. Therefore, it can be concluded that a large proportion of GABA and related compounds are transported via GAT-3. Residual uptake may be mediated by GAT-1.

A more detailed analysis of guvacine and (S)-SNAP 5114-mediated blocking of ALA and MAL uptake revealed closely similar apparent pK_i values for blocking ALA and MAL with both compounds, respectively (see Table 3).

One possibility to explain MAL-induced PpIX synthesis in neurones might arise from the presence of extracellular esterases hydrolysing MAL to ALA prior to the uptake. The addition of the highly hydrophilic, cell-impermeable, potent carboxyesterase inhibitor BNPP (Masaki et al. 2007) revealed a 23% reduction in PpIX formation from MAL. ALA-induced PpIX is at the same time unaltered or even slightly increased by BNPP. Thus, at least part of the PpIX formed in DRG neurones after MAL application may actually be ALA derived. Whether one organo-phosphate compound as BNPP is sufficient to deactivate all secreted esterases is, of course, debatable. Our results indicate that at least part of the MAL is hydrolyzed to ALA by extracellular esterase activity. Given the higher affinity of the resulting ALA to the transport systems, the amount of ALA formed by BNPP-sensitive esterases only represents a minor part of the MAL. If additional secreted esterases existed this could provide a possible explanation for MAL-induced PpIX in neurones.

Both ALA and MAL seem to enter neurones through GAT-3 and carrier systems for L-Arg. While this has already been suggested for ALA by Rud et al. (2000), the same authors also concluded that there was no effect of GAT substrates and polar amino acids on MAL uptake in adenocarcinoma cells (Gederaas et al. 2001). Similarly, we found that in keratinocytes (S)-SNAP-5114 fails to block MAL uptake at concentrations below 1 mM (unpublished observation). Several assumptions may explain this apparent inconsistency. It is conceivable that GAT-3 in neurons is post-translationally modified and thus different from GAT-3 in keratinocytes. Although such modifications have been postulated for CNS neurones (Patrylo et al. 2001), there is no evidence for this in the sensory nervous system.

Beyond the fact that MAL may partially be transported as ALA, the uptake pharmacology could be even more complex. We found pK_i values for (S)-SNAP 5114 at 3.7–3.9 and for guvacine at 2.6–2.8 (see Table 3). Borden et al. (1994) found pK_i values for these two compounds at GAT-3 that were

lower by one order of magnitude (SNAP: 5.3; guvacine: 3.9). At concentrations of 0.5 mM (*S*)-SNAP-5114 may block other transporters than just GAT-1 or GAT-3. In this case, ALA or MAL might be carried by such transporters. Unfortunately, there is no information on the pharmacological profile of (*S*)-SNAP-5114 on transporters other than those for GABA.

Alternatively, transporter expression differences between keratinocytes and DRG primary cultures may account for the difference. It is possible that in the absence of high-affinity carriers for MAL (which might be transporters for nonpolar amino acids), MAL might enter neurons via GAT, albeit with a lower affinity than ALA. In the presence of “better” transporters for MAL, such as in keratinocytes, it would almost entirely be taken up through those “better” transporters and not be detectably affected by competitors on GAT uptake.

If two systems for ALA transport were to exist, one challenged by polar amino acids (*L*-Arg) and one by GAT-3 substrates, and uptake were the rate-limiting step in PpIX synthesis, an additive effect could be envisaged. An additive effect could, however, not be confirmed by co-incubating the DRG cultures with β -alanine and *L*-Arg in combination with 0.6 mM ALA. The drug mixture only slightly increased the inhibition of PpIX formation compared to the individual competitors (by ca. 10%), and this increase was statistically insignificant. Further emphasis is required to unravel this inconclusive phenomenon, as no information is available on the effect of *L*-Arg on GABA transporters or of (*S*)-SNAP-5114 on amino acid carriers.

In summary, this study pioneers in characterising ALA and MAL uptake into sensory neurones, and defines GABA and/or amino acid transporters as the principal uptake pathways for both pro-drugs. PpIX production from MAL is lower due to reduced uptake, as also suggested for a variety of tumour lines. Part of the MAL may be hydrolyzed to ALA outside the cell. Any observations, describing lower painful side-effects of PDT after a 3-hour MAL incubation compared to a 6-hour ALA incubation (e.g. Kasche et al. 2006), are probably due to the different incubation times and the general deficit of MAL skin penetration and efficacy (Maisch et al. 2010) as opposed to an exclusive ALA uptake by sensory nerve fibres.

Acknowledgements The authors are indebted to the excellent technical support by Silvia Schweer and would also like to thank Xinran Zhu, Frank Paris, Beate Schmitz and Mirella Gwarek for many helpful discussions and inspirations. Special thanks to Anna Suedkamp and Mirella Gwarek for their kind help with the PpIX assay system and the radiolabelled GABA uptake experiments.

This work was supported with grants by the DFG (German research council) Graduiertenkolleg 736 and the Ruhr-University Bochum research school.

Conflict of interest One of the authors (HL) is closely linked as general manager to Biofrontera Bioscience GmbH which has a PDT drug containing ALA in the European approval process.

References

- Alexander SP, Mathie A, Peters JA (2009) Guide to Receptors and Channels (GRAC), 4th Edition. Br J Pharmacol 158(Suppl 1): S1–S254
- Almeida RD, Manadas BJ, Carvalho AP, Duarte CB (2004) Intracellular signaling mechanisms in photodynamic therapy. Biochim Biophys Acta 1704:59–86
- Andersen PL, Doucette JR, Nazarali AJ (2003) A novel method of eliminating non-neuronal proliferating cells from cultures of mouse dorsal root ganglia. Cell Mol Neurobiol 23:205–210
- Bermudez MM, Correa GS, Perotti C, Batlle A, Casas A (2002) Delta-Aminolevulinic acid transport in murine mammary adenocarcinoma cells is mediated by beta transporters. Br J Cancer 87:471–474
- Borden LA (1996) GABA transporter heterogeneity: pharmacology and cellular localization. Neurochem Int 29:335–356
- Borden LA, Dhar TG, Smith KE, Branchek TA, Gluchowski C, Weinschenk RL (1994) Cloning of the human homologue of the GABA transporter GAT-3 and identification of a novel inhibitor with selectivity for this site. Receptors Channels 2:207–213
- Casas A, Perotti C, Saccoliti M, Sacca P, Fukuda H, Batlle AM (2002) ALA and ALA hexyl ester in free and liposomal formulations for the photosensitisation of tumour organ cultures. Br J Cancer 86:837–842
- Cheng Y, Prusoff WH (1973) Relationship between the inhibition constant (K_1) and the concentration of inhibitor which causes 50 per cent inhibition (I_{50}) of an enzymatic reaction. Biochem Pharmacol 22:3099–3108
- Collaud S, Juzeniene A, Moan J, Lange N (2004) On the selectivity of 5-aminolevulinic acid-induced protoporphyrin IX formation. Curr Med Chem Anticancer Agents 4:301–316
- Conti F, Zuccarello LV, Barbaresi P, Minelli A, Brecha NC, Melone M (1999) Neuronal, glial, and epithelial localization of gamma-aminobutyric acid transporter 2, a high-affinity gamma-aminobutyric acid plasma membrane transporter, in the cerebral cortex and neighboring structures. J Comp Neurol 409:482–494
- Doring F, Walter J, Will J, Focking M, Boll M, Amasheh S, Clauss W, Daniel H (1998) Delta-aminolevulinic acid transport by intestinal and renal peptide transporters and its physiological and clinical implications. J Clin Invest 101:2761–2767
- Ericson MB, Sandberg C, Stenquist B, Gudmundson F, Karlsson M, Ros AM, Rosen A, Larko O, Wennberg AM, Rosdahl I (2004) Photodynamic therapy of actinic keratosis at varying fluence rates: assessment of photobleaching, pain and primary clinical outcome. Br J Dermatol 151:1204–1212
- Frolund S, Marquez OC, Larsen M, Brodin B, Nielsen CU (2010) Delta-aminolevulinic acid is a substrate for the amino acid transporter SLC36A1 (hPAT1). Br J Pharmacol 159:1339–1353
- Gaullier JM, Berg K, Peng Q, Anholt H, Selbo PK, Ma LW, Moan J (1997) Use of 5-aminolevulinic acid esters to improve photodynamic therapy on cells in culture. Cancer Res 57:1481–1486
- Gederaas OA, Holroyd A, Brown SB, Vernon D, Moan J, Berg K (2001) 5-Aminolaevulinic acid methyl ester transport on amino acid carriers in a human colon adenocarcinoma cell line. Photochem Photobiol 73:164–169
- Gilbert R, McNaughton P (1997) Enrichment of the fraction of nociceptive neurones in cultures of primary sensory neurones. J Neurosci Methods 71:191–198
- Grapengiesser S, Ericson M, Gudmundsson F, Larko O, Rosen A, Wennberg AM (2002) Pain caused by photodynamic therapy of skin cancer. Clin Exp Dermatol 27:493–497
- Hyde R, Taylor PM, Hundal HS (2003) Amino acid transporters: roles in amino acid sensing and signalling in animal cells. Biochem J 373:1–18

- Kasche A, Luderschmidt S, Ring J, Hein R (2006) Photodynamic therapy induces less pain in patients treated with methyl aminolevulinic acid compared to aminolevulinic acid. *J Drugs Dermatol* 5:353–356
- Kloek J, Akkermans W, Beijersbergen van Henegouwen GM (1998) Derivatives of 5-aminolevulinic acid for photodynamic therapy: enzymatic conversion into protoporphyrin. *Photochem Photobiol* 67:150–154
- Kragler A, Hofner G, Wanner KT (2005) Novel parent structures for inhibitors of the murine GABA transporters mGAT3 and mGAT4. *Eur J Pharmacol* 519:43–47
- Lawson SN (2002) Phenotype and function of somatic primary afferent nociceptive neurones with C-, Delta- or Aalpha/beta-fibres. *Exp Physiol* 87:239–244
- Lee JB, Choi JY, Chun JS, Yun SJ, Lee SC, Oh J, Park HR (2008) Relationship of protoporphyrin IX synthesis to photodynamic effects by 5-aminolevulinic acid and its esters on various cell lines derived from the skin. *Br J Dermatol* 159:61–67
- Lindeburg KE, Brogaard HM, Jemec GB (2007) Pain and photodynamic therapy. *Dermatology* 215:206–208
- Liu M, Russell RL, Beigelman L, Handschumacher RE, Pizzorno G (1999) beta-alanine and alpha-fluoro-beta-alanine concentrative transport in rat hepatocytes is mediated by GABA transporter GAT-2. *Am J Physiol* 276:G206–G210
- Lumpkin EA, Caterina MJ (2007) Mechanisms of sensory transduction in the skin. *Nature* 445:858–865
- MacCormack MA (2008) Photodynamic therapy in dermatology: an update on applications and outcomes. *Semin Cutan Med Surg* 27:52–62
- Maisch T, Santarelli F, Schreml S, Babilas P, Szeimies RM (2010) Fluorescence induction of protoporphyrin IX by a new 5-aminolevulinic acid nanoemulsion used for photodynamic therapy in a full-thickness ex vivo skin model. *Exp Dermatol* 19:e302–e305
- Malin SA, Davis BM, Molliver DC (2007) Production of dissociated sensory neuron cultures and considerations for their use in studying neuronal function and plasticity. *Nat Protoc* 2:152–160
- Masaki K, Hashimoto M, Imai T (2007) Intestinal first-pass metabolism via carboxylesterase in rat jejunum and ileum. *Drug Metab Dispos* 35:1089–1095
- Minelli A, Barbaresi P, Conti F (2003) Postnatal development of high-affinity plasma membrane GABA transporters GAT-2 and GAT-3 in the rat cerebral cortex. *Brain Res Dev Brain Res* 142:7–18
- Novotny A, Xiang J, Stummer W, Teuscher NS, Smith DE, Keep RF (2000) Mechanisms of 5-aminolevulinic acid uptake at the choroid plexus. *J Neurochem* 75:321–328
- Passmore GM (2005) Dorsal root ganglion neurones in culture: a model system for identifying novel analgesic targets? *J Pharmacol Toxicol Methods* 51:201–208
- Patrylo PR, Spencer DD, Williamson A (2001) GABA uptake and heterotransport are impaired in the dentate gyrus of epileptic rats and humans with temporal lobe sclerosis. *J Neurophysiol* 85:1533–1542
- Priestley JV, Michael GJ, Averill S, Liu M, Willmott N (2002) Regulation of nociceptive neurons by nerve growth factor and glial cell line derived neurotrophic factor. *Can J Physiol Pharmacol* 80:495–505
- Riopelle RJ, Kennedy JC (1982) Some aspects of porphyrin neurotoxicity in vitro. *Can J Physiol Pharmacol* 60:707–714
- Rodriguez L, Batlle A, Di Venosa G, Battah S, Dobbin P, MacRobert AJ, Casas A (2006) Mechanisms of 5-aminolevulinic acid ester uptake in mammalian cells. *Br J Pharmacol* 147:825–833
- Rud E, Gederaas O, Hogset A, Berg K (2000) 5-aminolevulinic acid, but not 5-aminolevulinic acid esters, is transported into adenocarcinoma cells by system BETA transporters. *Photochem Photobiol* 71:640–647
- Sarup A, Larsson OM, Schousboe A (2003) GABA transporters and GABA-transaminase as drug targets. *Curr Drug Targets CNS Neurol Disord* 2:269–277
- Schmidt S, Linnartz B, Mendritzki S, Sczepan T, Lubbert M, Stichel CC, Lubbert H (2011) Genetic mouse models for Parkinson's disease display severe pathology in glial cell mitochondria. *Hum Mol Genet* 20:1197–1211
- Shoji Y, Yamaguchi-Yamada M, Yamamoto Y (2010) Glutamate- and GABA-mediated neuron-satellite cell interaction in nodose ganglia as revealed by intracellular calcium imaging. *Histochem Cell Biol* 134:13–22
- Stucky CL, Lewin GR (1999) Isolectin B(4)-positive and -negative nociceptors are functionally distinct. *J Neurosci* 19:6497–6505
- Tunstall RG, Barnett AA, Schofield J, Griffiths J, Vernon DI, Brown SB, Roberts DJ (2002) Porphyrin accumulation induced by 5-aminolevulinic acid esters in tumour cells growing in vitro and in vivo. *Br J Cancer* 87:246–250
- Uehlinger P, Zellweger M, Wagnieres G, Juillerat-Jeanneret L, van den Bergh H, Lange N (2000) 5-Aminolevulinic acid and its derivatives: physical chemical properties and protoporphyrin IX formation in cultured cells. *J Photochem Photobiol B* 54:72–80
- Van Hillegersberg R, Van den Berg JW, Kort WJ, Terpstra OT, Wilson JH (1992) Selective accumulation of endogenously produced porphyrins in a liver metastasis model in rats. *Gastroenterology* 103:647–651
- Vitellaro-Zuccarello L, Calvaresi N, De Biasi S (2003) Expression of GABA transporters, GAT-1 and GAT-3, in the cerebral cortex and thalamus of the rat during postnatal development. *Cell Tissue Res* 313:245–257
- Vyklicky L, Knotkova-Urbancova H (1996) Can sensory neurones in culture serve as a model of nociception? *Physiol Res* 45:1–9
- Washbrook R, Fukuda H, Battle A, Riley P (1997) Stimulation of tetrapyrrole synthesis in mammalian epithelial cells in culture by exposure to aminolevulinic acid. *Br J Cancer* 75:381–387
- Wendt W, Zhu XR, Lubbert H, Stichel CC (2007) Differential expression of cathepsin X in aging and pathological central nervous system of mice. *Exp Neurol* 204:525–540
- Wennberg AM, Larko O, Lonnroth P, Larson G, Krogstad AL (2000) Delta-aminolevulinic acid in superficial basal cell carcinomas and normal skin—a microdialysis and perfusion study. *Clin Exp Dermatol* 25:317–322
- Whitaker CJ, Battah SH, Forsyth MJ, Edwards C, Boyle RW, Matthews EK (2000) Photosensitization of pancreatic tumour cells by delta-aminolevulinic acid esters. *Anticancer Drug Des* 15:161–170